NCHRP Web Document 36 (Project D10-37A[1]): Contractor's Final Report

Extended Exposure and Monitoring of Epoxy-Coated Reinforced Concrete Test Slabs

Prepared for:

National Cooperative Highway Research Program
Transportation Research Board
National Research Council

Submitted by:

William H. Hartt
S. K. Lee
Center for Marine Materials
Department of Ocean Engineering
Florida Atlantic University—Sea Tech Campus
Dania Beach, Florida

May 2001

ACKNOWLEDGMENT

This work was sponsored by the American Association of State Highway and Transportation Officials (AASHTO), in cooperation with the Federal Highway Administration, and was conducted in the National Cooperative Highway Research Program (NCHRP), which is administered by the Transportation Research Board (TRB) of the National Research Council.

CONTENTS

EXTENDED EXPOSURE AND MONITORING OF EPOXY-COATED REINFORCED CONCRETE TEST SLABS

SUMMARY

A total of 76 salt contaminated concrete slabs that contained epoxy-coated reinforcement (ECR) were fabricated in October, 1992 and exposed outdoors beginning in March, 1993 in Boca Raton, Florida as a part of NCHRP Project 10-37. Exposure of the slabs was terminated and autopsies were performed at various subsequent times with the last remaining slabs being removed from testing in November, 1999 after over six years. The epoxy-coated bars were acquired from six different sources and were characterized initially in terms of 1) coating thickness, hardness, and defect density and 2) performance in several accelerated tests. During the first 2.7 years of exposure, the slabs were subjected to four different potable water wet-dry ponding cycles. Subsequently, all slabs experienced natural weathering only but with some being subjected to predominantly wet ponding with a 15 percent NaCl solution during the final 13 months. Monitoring involved periodic measurement of potential, macrocell current, and impedance @ 0.1 Hz.

Upon autopsy, condition of the ECRs was assessed; and performance of the slabs was found to correlate with the density of initial coating defects, which may reflect coating quality, and with exposure severity (natural weathering versus natural weathering plus salt water ponding). Additional coating defects formed during the course of the exposure at a rate that was 1) constant with time and 2) proportional to the number of initial defects. The rate at which such defects formed was approximately seven times higher with salt water ponding compared to natural weathering. Coating disbondment, which provided direct electrolyte access to the steel and led to corrosion, occurred in proportion to the defect density. In general, corrosion rate for bars was relatively low and was independent of coating defect density as long as this density remained below approximately one defect per inch of bar length, whereas corrosion rate was higher and increased in proportion to defect density above this.

A model for predicting service life of the ECR reinforced concrete slabs was developed assuming that this was comprised of three component periods. The first of these was the time for a threshold concentration of chlorides to accumulate at the steel depth (this time was nil for the present slabs since these were chloride admixed; however, it could be significant for actual structures), the second was the time subsequent to chloride accumulation for a coating defect density of one per inch to develop on the ECRs, and the third was the time subsequent to occurrence of a defect density of one per inch for a net corrosion wastage of one mil (approximately two $\mu A \cdot$ years of charge transfer) to develop. The results indicated that the time to significant corrosion and corrosion induced concrete cracking and spalling subsequent to chloride contamination decreased from 46 to 16 years for the natural weathering exposure and from about 6.5 to 2.0 years for the salt water ponding as the density of initial coating defects increased from the present specification value of one per foot to one per inch. Such a result for the salt water ponded slabs is consistent with the Florida Keys bridges substructure experience, indicating an apparent equivalence in the two exposures. On the other hand, environmental exposure severity for northern bridge decks subject to deicing salts may be more equivalent to the natural weathering exposure and, here, ECR performance should vary according to temperature, time of wetness, and frequency of salt applications. The fact that a recent study reported an average in-place ECR coating defect density of approximately one per inch for newly constructed

bridge decks indicates that the second of the three above time periods is nil for 50 percent of these structures such that a service life of 25 years subsequent to chloride contamination applies.

It is recommended that a study be commissioned to expand the service life model from the two discrete exposures (salt water ponding and natural weathering) to a continuum and calibrate this with North American longitudes and latitudes and salting practice. A companion study is recommended to determine the coating defect density for bars in existing bridges as a function of age and exposure severity as defined by the variables of temperature, time-of-wetness, concrete chloride concentration, and frequency of salt applications. Also, recommended is that efforts by states to enhance long-term durability of ECR reinforced concrete focus upon methods whereby 1) the time to occurrence of the threshold chloride concentration at the steel depth can be increased and 2) the coating defect density of in-place ECRs for new construction can be reduced.

CHAPTER 1

INTRODUCTION AND RESEARCH APPROACH

Corrosion of steel in concrete has evolved over the past three decades to become the single most costly corrosion problem in the United States. As a consequence, research programs pertaining to such deterioration have been conducted by, in addition to the National Cooperative Highway Research Program (NCHRP), the Federal Highway Administration (FHWA), National Institute of Standards and Technology (NIST), American Association of State Highway and Transportation Officials (AASHTO), and state transportation agencies. In this regard, research by NIST (1) and FHWA (2) indicated that powdered epoxy-coated reinforcing steel (ECR) performed well in salt contaminated concrete; and based upon these results, the North American highway community has extensively employed this material in bridges since the mid-1970s.

Initial questioning of the utility of epoxy-coatings upon reinforcing steel for providing long-term corrosion protection to concrete structures exposed to chloride environments arose in the mid-1080s in conjunction with appearance of cracking and spalling of various bridge substructure members in the Florida Keys after only six years service (3-6). Corrosion was initially observed in areas that contained fabricated (bent) ECRs, but eventually straight bars as well were found to be deteriorated. These members are located in and adjacent to the splash zone and, thus, are subjected to salt spray and repeated cycles of wetting and drying. Relatively high air and water temperatures also contribute to the harshness of this exposure. Other instances of unsatisfactory ECR performance have subsequently been reported (7,8).

In 1991, the NCHRP commissioned a comprehensive research study (NCHRP Project Number 10-37) to investigate the cause(s) for unsatisfactory performance of epoxy-coated reinforcing steel, where this had occurred in highway bridges, and to make recommendations for improvements to current practice and specifications that pertain to this technology. A comprehensive report that details the findings of this study has been published (9). As a component of this investigation, 88 concrete test slabs, 76 of which contained ECRs and 12 of which were controls (black reinforcement only), were fabricated in October, 1992 by K. C. Clear, Inc. These were subsequently cured for 30 days, delivered to Florida Atlantic University, demolded, epoxy coated on the four sides, and exposed on elevated racks in a test yard approximately three km (2 miles) from the Atlantic Ocean in Boca Raton, Florida.

Because of the relatively brief exposure that the Project 10-37 ECR test slabs had experienced within the timeframe of that project (10 months), a decision was made to only autopsy and report on the condition of seven of these plus one control and to continue the exposure and monitoring of the remaining slabs. This continued activity was accomplished under the auspices of NCHRP Projects 10-37A and 10-37D. In addition to the initial autopsy of eight specimens during Project 10-37, two subsequent autopsies were conducted as a part of Project 10-37A, the first upon three slabs in December, 1995 and the second upon 22 slabs in May, 1996. Exposure of the remaining 44 slabs continued under Project 10-37D, and these were all autopsied in December, 1999. Appendix A provides background information regarding the ECRs, fabrication of the concrete slabs, the exposure test program, and the autopsy procedure. The purpose of this report is to 1) present data from the Project 10-37A exposure periods, 2) present

findings from the specimen autopsies, 3) analyze and summarize results for the 76 ECR slabs, and 4) draw conclusions regarding long-term performance of ECRs in chloride contaminated reinforced concrete bridge applications.

CHAPTER 2

FINDINGS

AUTOPSY RESULTS

GENERAL

Table 1 presents data and results for the second and third autopsies and Table 2 for the fourth. Results from the initial autopsy of seven ECR slabs after ten months exposure were reported previously (9) and provided no useful information to the final analysis, and so these have not been repeated here.

CONDITION OF SLABS

Fine hairline cracks were detected on the top surface of some of the slabs along the rebar trace in June, 1995. Similar cracks were apparent upon the control (black bar) specimens at the time they were received at FAU (December, 1992). The second autopsy (December, 1995) was performed upon three ECR slabs with hairline cracks to determine the cause of these. This revealed no correlation between the magnitude of corrosion and the presence and extent of cracking.

The present investigators have been involved with several projects subsequent to the present one where concrete slabs reinforced with black bars were cast. Cover over the reinforcement in these cases ranged from 19 to 32 mm (0.75 to 1.25 in). In all cases, subsidence cracks developed along the upper bars as the concrete set. It is thought that this same phenomenon occurred in the present black bar slabs and to an initially undetectable extent in the ECR ones. These cracks in the black bar slabs were wider at the time they were received, which was about two months after fabrication, than for the ECR slabs several years later. Once ponding commenced, water had direct access to reinforcement in the black bar slabs. This resulted in widening of the existing cracks and development of additional cracks to such an extent that the concrete eventually fell apart. Because cracks were present in these specimens prior to exposure, it was considered inappropriate to quantify performance of these relative to the ECR slabs. However, it was apparent that the ECRs were much more tolerant to the presence of cracks than were the black bars, as evidenced by the fact that none of the slabs with ECRs exhibited 1) cracks that could be attributed to corrosion or 2) spalling; and certainly, none of these slabs fell apart as did the black bar ones.

Presence of the concrete cracks in the ECR slabs provided a unique opportunity to study performance under conditions encountered in practice, since such cracks commonly occur directly above ECRs in bridge decks. These cracks extended and widened with time with the rate at which this occurred being most advanced during the 13 month salt water ponding period. Table 3 provides a summary of the extent of cracking as of December, 1997 and November, 1999 for specimens that remained at the time of the final autopsy. This indicates that the average crack extension during the two years between which these measurements were made was 15 percent for the natural weathering slabs and 42 percent for the ponded ones. It was concluded that the salt water ponding contributed to an accelerated cracking rate; however, because no correlation was apparent between the extent of ECR corrosion and cracking, it is not clear that corrosion per se was responsible. During autopsies, it was determined that the ECR-concrete bond was sufficiently weak that the bars could be easily removed by hand from the sectioned concrete.

Table 1: Properties and performance data for ECRs extracted from slabs autopsied during the second and third autopsies.

Category	Spec. ID	Source	Exposure	No. of Initial Defects	No. of Final Defects	Disbond., percent	Adhesion	log[Z] @0.1 Hz ('95)	log[Z] @0.1 Hz ('96)	OCP, (V vs SCE) ('93)	CURRENT,µA ('93)	OCP, (V vs SCE) ('95)	CURRENT,µA ('95)	OCP, (V vs SCE) ('96)	CURRENT, mA ('96)	Cl-, ppm
	1L	N	A	2	Line of cut	16.9	Moderate	4.751	4.799	-0.130	1.50E+01	-0.231	2.00E-02	-0.207	1.25E+00	
	1R	N	A	6	8	10.1	Moderate	5.241	5.836	-0.182		-0.205	1.00E-06	-0.142	-1.00E-05	
	2L	N	B	14	16	28.4	Moderate	4.316	4.546	-0.124	7.20E+01	-0.091	9.00E-02	-0.057	3.70E-04	
	2R	N	B	9	7	25.0	Moderate	4.298	4.564	-0.218		-0.089	6.00E-02	-0.052	9.00E-01	
	13L	J	A	0	3	0.0	Moderate	6.464	6.525	-0.068	7.00E+00	-0.081	1.00E-02	-0.115	2.00E-05	
	13R	J	A	3	5	3.7	Moderate	5.486	5.571	-0.271		-0.119	1.00E-06	-0.175	4.10E-04	
	17L	J	A	5	16	17.6	Moderate	3.782	4.071	-0.250	6.30E+01	-0.160	2.10E-01	-0.180	2.50E+00	
	17R	J	A	1	14	2.9	Moderate	6.094	6.184	-0.193		-0.129	1.00E-06	-0.145	1.00E-05	
	19L	J	C	4	ED**	20.6	Moderate	3.524	3.950	-0.491	1.09E+02	-0.285	5.60E+00	-0.108	1.23E+00	
	19R	J	C	2	10	4.4	Good	6.533	6.473	-0.231		-0.135	1.00E-06	-0.101	2.00E-04	
	21L	J	A	2	6	2.2	Good	4.786	4.236	-0.070	1.00E-06	-0.133	5.00E-02	-0.170	3.00E+00	2980
	21R	J	A	3	10	2.2	Poor	4.489	4.520	-0.075		-0.132	5.00E-02	-0.210	5.70E-02	1332
	23L	J	C	1	6	0.0	Moderate	6.538	7.465	0.020	1.00E-06	-0.414	1.00E-06	-0.139	5.00E-05	2555
	23R	J	C	1	4+ LDA*	17.6	Moderate	3.244	3.705	0.031		-0.187	6.10E-02	-0.132	1.14E+00	2515
	32L	A	D	6	12	7.6	Poor	4.040	4.124	-0.115	7.00E+00	-0.334	2.71E+00	-0.189	3.40E-01	
	32R	A	D	4	12	3.0	Poor	4.650	4.623	-0.114		-0.107	5.00E-02	-0.178	5.00E-04	
	33L	A	A	0	2	1.5	Poor	6.052	5.921	-0.100	1.00E-06	-0.105	1.00E-02	-0.088	-8.00E-05	
	33R	A	A	0	1	0.0	Poor	7.272	7.242	-0.096		-0.060	1.00E-06	-0.054	-0.00004	
3rd	38L	A	B	2	3	5.3	Moderate	4.870	4.474	-0.124	1.70E+01	-0.063	2.00E-02	-0.060	4.20E-01	
Autopsy	38R	A	B	1	12	1.5	Poor	6.440	7.012	-0.121		-0.052	1.00E-06	-0.002	-0.00018	
Non-Pre-	42L	D	B	4	8	3.4	Good	5.724	6.340	0.174	8.00E+00	-0.055	1.00E-06	-0.042	1.50E-04	3013
Weathered	42R	D	B	0	5	4.1	Moderate	5.621	6.519	0.140		-0.056	1.00E-06	-0.038	1.10E-04	2524
ECRs	44L	D	D	0	1	0.0	Good	6.629	6.861	0.039	3.00E+00	-0.077	1.00E-06	-0.001	1.40E-04	2786
	44R	D	D	2	2	2.7	Good	4.616	4.636	0.037		-0.125	1.00E-02	-0.002	7.50E-02	2992
	51L	D	C	0	3	2.0	Moderate	5.994	7.045	-0.176	1.00E-06	-0.130	1.00E-02	-0.080	5.00E-05	
	51R	D	C	0	0	0.0	Moderate	7.336	8.327	-0.016		-0.064	1.00E-06	-0.013	-1.30E-04	
	55L	T	C	80	3+ LDA*	98.6	Zero	3.027	2.987	-0.288	4.70E+02	-0.264	1.69E+01	-0.119	5.90E+00	2260
	55R	T	C	42	18+ LDA*	100.0	Zero	3.579	3.817	-0.217		-0.230	9.30E-01	-0.118	7.40E-01	62***
	57L	T	A	34	67	90.3	Zero	4.048	4.192	-0.110	6.50E+01	-0.125	5.00E-01	-0.167	2.20E+01	
	57R	T	A	8	21	15.3	Poor	4.447	4.571	-0.136		-0.118	5.00E-02	-0.151	9.20E-04	
	58L	T	B	18	49+ LDA*	90.0	Zero	3.865	3.931	-0.143	1.28E+02	-0.145	3.00E-01	-0.120	1.27E+00	2986
	58R	T	B	27	70	79.2	Zero	3.566	3.617	-0.161		-0.140	1.77E+00	-0.076	3.50E+00	3158
	59L	T	C	11	33	34.7	Good	4.262	4.773	-0.138	3.30E+01	-0.221	2.20E-01	-0.136	1.40E-03	
	59R	T	C	5	55	72.2	Good	3.806	4.005	-0.156		-0.205	6.10E+00	-0.144	4.60E-01	
	60L	T	D	23	62	94.4	Zero	3.700	3.730	0.175	7.20E+01	-0.067	3.90E-01	-0.061	2.40E+00	2809
	60R	T	D	69	ED**	83.3	Zero	3.604	3.517	0.001		-0.068	2.60E-01	-0.067	2.30E+00	3120
	65L	U	A	0	1	0.0	Moderate	6.765	7.052	-0.125	1.00E-06	-0.070	1.00E-06	-0.116	7.00E-05	3547
	65R	U	A	1	2	0.0	Poor	6.732	6.793	-0.168		-0.080	1.00E-06	-0.068	5.00E-05	340***
	72L	U	D	0	0	0.0	Moderate	5.500	5.687	0.040	1.00E-06	-0.043	1.00E-06	-0.047	2.50E-04	
	72R	U	D	0	3	2.3	Good	5.690	6.498	0.074		-0.001	1.00E-06	-0.043	9.00E-05	
	79L	CONTROL	C	N/A	N/A	N/A	N/A	N/A	N/A	-0.406	1.05E+03	-0.582	4.59E+02	-0.222	8.00E+01	1469
	79R	CONTROL	C	N/A	N/A	N/A	N/A	N/A	N/A	-0.358		-0.605	5.45E+02	-0.235	1.51E+02	1849
	10RR	NUV	D	1	11	37.5	Good	5.363	4.996	-0.297		-0.332	4.40E-01	-0.110	1.07E-03	
	10RF	NUV	D	0	13	45.8	Good	5.286	4.932	-0.281	7.00E+00	-0.110	5.00E-02	-0.096	1.30E+00	
3rd	10LR	NUV	D	0	21	66.7	Zero	4.783	4.170	0.081		-0.478	4.30E-01	-0.099	4.60E-01	
Autopsy	10LF	NUV	D	1	6	37.5	Good	5.043	4.562	0.053		-0.115	3.00E-02	-0.100	1.42E+00	
Pre-	25RR	JUV	A	0	17	16.7	Good	5.707	5.843	-0.095		-0.215	5.00E-02	-0.345	7.50E-04	
Weathered	25RF	JUV	A	0	6	12.5	Poor	4.788	5.388	-0.105	6.00E+00	-0.257	2.50E-01	-0.007	3.20E-01	
ECRs	25LR	JUV	A	0	0	0.0	Good	6.712	5.653	-0.117		-0.121	1.00E-06	-0.160	3.90E-04	
	25LF	JUV	A	1	80	45.8	Good	3.806	3.715	-0.087		-0.254	1.23E+00	-0.224	2.00E+01	
	24L	J	D	9	13	8.8	Moderate		4.358	0.066	2.40E+01	-0.158	1.00E-06			
	24R	J	D	0	1	0.0	Moderate		6.551	0.090		-0.085	2.20E-01			
2nd	35L	A	C	0	12	1.5	Moderate		6.367	0.043	1.00E-06	-0.099	1.00E-06			
Autopsy	35R	A	C	0	4	0.0	Moderate		7.410	0.059		-0.074	1.00E-06			
ECRs	64L	T	D	23	36	63.9	Moderate		3.367	-0.066	1.27E+02	-0.092	6.00E-01			
	64R	T	D	43	ED**	100.0	Zero		3.092	0.164		-0.087	1.77E+00			

* LDA : Localized Damage Areas

** ED : Excessive Defects

*** Chloride content at 25 mm (1 in.) above bottom m

+: Number indicates slab designation (L - Left ECR, R - Right ECR

Table 2: Properties and behavior of ECRs extracted from slabs during the fourth autopsy.

Group I: Ponded specimens with 15 wt.% NaCl solution for the last 13 months prior to autopsy

ECR ID	Source	Initial Defects		Final Defects					Disbond'g	Knife	OCP (V, SCE)				Macrocell current (uA)				log [Z] @ 0.1 Hz				[Cl]-	[Cl]-
		Mashed	# Beeps	Bare	Crack	Holiday	Blister	Total	(%)	Adhesion	Initial (4/93)	3/95	5/98	Final (11/99)	Initial (4/93)	3/95	5/98	Final (11/99)	Initial (2/93)	3/95	10/98	Final (11/99)	Top	Bottom
5L	N	2	6	8	21	0	0	29	46	M	-0.147	-0.163	-0.163	-0.597	1.500	0.8900	1.3600	22.8000		1.1E+04	1.6E+04	1.7E+03	13008	
5R	N	4	5	7	16	0	0	23	60	M	-0.207	-0.15	-0.034	-0.618		0.0500	0.9540	31.4000		4.0E+04	5.7E+04	2.1E+03		
7L	N	6	3	4	6	1	0	11	12.5	M	-0.096	-0.101	-0.006	-0.585	0.000	0.0200	0.0001	31.7000		6.5E+05	6.2E+05	8.3E+03		
7R	N	10	11	Excessive Damages					66	M	-0.102	-0.134	-0.01	-0.588		0.0001	0.0010	119.5000		3.9E+04	3.5E+04	9.5E+02	17326	
16L	J	4	1	1	48	0	0	49	30	G	-0.082	-0.192	-0.195	-0.637	0.280	1.0700	-0.3220	80.8000	8.7E+03	3.1E+04	9.2E+04	1.9E+03		
16R	J	3	0	Excessive Damages					50	P	-0.086	-0.099	-0.14	-0.681		0.0200	-0.1390	148.2000	2.1E+05	3.9E+05	3.7E+05	9.7E+02	15173	
29L	A	0	5	6	43	0	0	49	38	M	-0.097	-0.213	-0.222	-0.694	0.160	0.2600	0.7680	85.7000		8.7E+04	1.1E+05	9.9E+02	13960	
29R	A	0	0	0	11	0	0	11	9	M	-0.303	-0.249	-0.152	-0.703		0.0700	0.0001	9.2000		3.0E+06	4.2E+07	8.6E+03		
31L	A	2	1	2	7	2	0	11	12	M	-0.076	-0.046	-0.052	-0.256	0.030	0.0001	0.0001	0.0001		7.3E+06	1.0E+07	2.6E+06	16437	6018
31R	A	5	5	Excessive Damages					94	Z	-0.031	-0.053	-0.14	-0.633		0.0001	0.0010	203.0000		1.0E+07	4.3E+04	1.9E+02		
36L	A	0	0	1	18	2	0	21	35	M	-0.113	-0.028	-0.095	-0.631	6.600	0.0900	0.0001	18.8000	4.0E+04	2.1E+05	4.0E+05	1.1E+04	17056	
36R	A	2	16	Excessive Damages					60	M	-0.403	-0.025	-0.139	-0.534		0.7100	0.4870	202.0000	7.7E+03	4.6E+03	2.1E+04	7.9E+02		
40L	A	0	2	0	12	0	0	12	12	P	-0.046	-0.035	-0.139	-0.686	0.020	0.0001	0.0001	50.6000		6.9E+06	4.8E+06	3.7E+03		956
40R	A	3	2	Excessive Damages					33	P	-0.115	-0.12	-0.249	-0.663		0.0001	1.0610	270.0000		1.9E+05	3.9E+04	6.2E+02	14110	
41L	D	4	0	1	16	0	0	17	15	M	-0.15	-0.102	-0.141	-0.744	0.070	0.0001	0.0001	8.1000	4.9E+05	1.8E+06	4.5E+05	1.1E+04		
41R	D	0	1	10	3	0	0	13	9	G	-0.118	-0.113	-0.092	-0.502		0.0001	0.0001	3.0000	7.7E+04	1.2E+06	9.6E+05	2.4E+04	14358	
43L	D	0	0	4	13	1	0	18	23	G	-0.099	-0.206	-0.094	-0.566	0.360	0.0500	0.0410	4.7000		1.0E+05	2.3E+05	4.4E+03		5890
43R	D	3	0	0	2	0	0	2	7	M	-0.073	-0.196	-0.036	-0.588		0.0600	-0.0020	-1.4000		1.1E+06	1.7E+06	2.6E+04	15787	
48L	D	3	3	3	3	0	0	6	16	G	-0.085	-0.095	-0.04	-0.484	0.040	0.0001	0.0001	2.4300		4.5E+05	7.3E+05	1.2E+04		
48R	D	3	4	8	21	0	0	29	26	G	-0.001	-0.088	-0.013	-0.515		0.0001	-0.1970	8.3600		2.6E+05	8.2E+04	4.5E+03	12282	
52L	D	5	1	2	2	0	1	5	8.5	G	-0.065	-0.12	-0.043	-0.419	0.000	0.0001	0.0001	40.0000		9.1E+05	N/A	9.2E+03		
52R	D	5	1	10	42	4	2	58	39	G	-0.038	-0.114	-0.07	-0.618		0.0100	6.2200	22.1000		1.2E+05	4.7E+03	9.5E+02	14911	
53L	T	3	4	24	58	0	3	85	99	Z	-0.044	-0.139	-0.135	-0.582	3.700	0.0500	-0.4310	32.6000	1.4E+04	9.6E+04	4.7E+04	1.5E+03		
53R	T	2	12	27	32	0	1	60	93	Z	-0.275	-0.151	-0.122	-0.548		0.8200	-1.8310	18.8000	2.9E+03	8.9E+03	6.1E+03	1.5E+03	11941	
63L	T	4	16	Excessive Damages					100	Z	-0.227	-0.254	-0.146	-0.655	N/A?	2.7000	-3.2110	660.0000		3.8E+03	3.3E+03	1.9E+02	12761	3540
63R	T	5	60	Excessive Damages					100	Z	-0.034	-0.298	-0.159	-0.709		24.9000	0.9570	333.0000		7.3E+02	2.0E+03	1.5E+02		
66L	U	1	0	0	5	0	0	5	1	G	-0.077	-0.115	-0.14	-0.537	0.000	0.0200	0.0001	1.2000		8.4E+05	2.4E+06	4.7E+04	9757	
66R	U	1	6	0	5	1	0	6	1	P	-0.078	-0.098	-0.13	-0.522		0.0200	0.0001	3.3000		2.0E+05	8.7E+05	4.7E+04		
68L	U	0	0	0	0	0	0	0	0	M	-0.02	-0.042	-0.1	-0.580	0.000	0.0001	0.0001	28.9000		3.2E+06	5.2E+06	5.7E+03	14751	
68R	U	0	1	1	3	2	0	6	12.5	M	-0.074	-0.048	-0.068	-0.654		0.0001	0.0010	7.5000		4.3E+05	2.0E+06	1.3E+04		
71L	U	0	0	0	3	1	0	4	4	G	-0.082	-0.115	-0.176	-0.614	0.080	0.0001	0.0001	4.3000	2.4E+05	6.5E+06	2.1E+06	5.2E+04		
71R	U	0	2	1	6	0	0	7	10	M	-0.087	-0.145	-0.189	-0.626		0.0200	-0.0020	4.1000	4.3E+04	1.5E+05	1.4E+05	1.9E+04	13838	
73L	U	0	0	1	7	0	0	8	3	P	-0.019	N/A	-0.276	-0.660	0.050	N/A	0.0001	20.4000		1.3E+07	1.2E+05	5.2E+03		1264
73R	U	1	1	0	3	0	0	3	1	P	-0.08	-0.095	-0.104	-0.619		0.0001	0.0001	1.4000		1.1E+06	2.5E+05	6.2E+04	12703	

Group II: Specimens exposed to natural weathering for the last 13 months prior to autopsy

3L	N	4	5	6	0	0	0	6	18	P	-0.062	-0.199	-0.092	-0.097	1.700	0.0400	0.2170	0.0040	4.7E+04	2.5E+05		9.2E+04		
3R	N	1	15	16	11	0	0	27	48	M	-0.118	-0.271	-0.121	-0.038		0.9700	1.8590	0.0800	3.9E+03	6.9E+03		9.4E+03	3365	
6L	N	2	3	4	3	0	0	7	16	G	-0.095	-0.106	-0.123	-0.158	4.100	0.0200	0.3360	-0.2500		6.2E+04		3.9E+04		
6R	N	0	2	2	8	0	0	10	20	M	-0.089	-0.119	-0.055	-0.090		0.2500	0.0010	-0.0003		2.1E+05		5.3E+04		
8L	N	3	5	6	4	1	0	11	16	P	-0.069	-0.11	-0.006	-0.149	0.100	0.0100	0.0010	-0.0004		3.0E+06		3.8E+04		
8R	N	2	0	1	0	0	0	1	0	M	-0.115	-0.078	-0.063	-0.148		0.0001	0.0010	-0.0410		6.5E+04		3.5E+04	1875	
9FL	NUV	2	0	0	15	0	0	15	33	G	-0.096	-0.111	-0.159	-0.128	0.080	0.0001	0.0010	-0.2000	1.1E+05	3.9E+05		1.8E+04		
9FR	NUV	0	0	0	8	0	0	8	15	M	-0.14	-0.12	-0.255	-0.246		0.0001	0.0001	0.0009	9.1E+04	3.3E+05		3.8E+05		
9RL	NUV	3	0	0	12	0	0	12	21	G	-0.062	-0.238	-0.324	-0.228		0.3400	0.8460	0.0010	1.5E+05	1.3E+03		6.3E+04		
9RR	NUV	0	0	0	6	0	0	6	6	M	-0.062	-0.135	-0.361	-0.253		0.0300	0.1760	0.0006	6.2E+05	1.6E+05		7.2E+05		
11FL	NUV	0	0	0	3	0	0	3	27	G	-0.297	-0.491	-0.136	-0.209	1.300	0.9800	0.0010	0.3000		2.8E+05		3.4E+04		
11FR	NUV	1	0	0	1	0	0	1	2	G	-0.106	-0.292	-0.25	-0.228		0.1000	0.2630	0.0007		7.8E+05		1.9E+05		387
11RL	NUV	0	2	1	5	0	0	6	62	G	-0.116	-0.313	-0.182	-0.215		0.7000	0.0010	-0.0003		1.4E+05		2.5E+05	2559	
11RR	NUV	0	0	0	3	0	0	3	8	G	-0.363	-0.352	-0.123	-0.146		1.7300	0.0010	0.0003		4.1E+05		5.0E+05		

*Knife adhesion: G (Good), M (Moderate), P (Poor), and Z (Zero testable area). ** N/A: Not Available. ***N/A? indicates uncertainty in data.

Table 2: Properties and behavior of ECRs extracted from slabs during the fourth autopsy.

ECR ID	Source	Initial Defects		Final Defects					Disbond'g	Knife	OCP (V, SCE)				Macrocell current (uA)				log [Z] @ 0.1 Hz				[Cl]-	[Cl]-
		Mashed	# Beeps	Bare	Crack	Holiday	Blister	Total	(%)	Adhesion	Initial (4/93)	3/95	5/98	Final (11/99)	Initial (4/93)	3/95	5/98	Final (11/99)	Initial (2/93)	3/95	10/98	Final (11/99)	Top	Bottom
12FL	NUV	0	0	0	1	0	0	1	6	G	-0.124	-0.13	-0.306	-0.040	0.430	0.0001	0.0010	-0.0003		4.5E+05		1.7E+07		
12FR	NUV	0	0	0	2	0	0	2	42	M	-0.163	-0.122	-0.104	-0.159		0.0600	0.0001	-0.0003		9.1E+04		2.8E+05	2021	
12RL	NUV	1	0	1	2	0	0	3	10	G	-0.124	-0.501	-0.455	-0.442	0.430	0.0100	0.6010	1.0000		8.9E+05		8.6E+05		
12RR	NUV	0	0	0	2	0	0	2	32	G	-0.204	-0.384	-0.301	-0.216		0.0100	0.4830	0.0005		3.8E+05		6.4E+05		
15L	J	5	0	2	5	0	0	7	3	G	-0.055	-0.126	-0.154	-0.246	0.080	0.0001	0.0010	0.1000	5.7E+04	1.3E+06		4.4E+04		416
15R	J	4	3	Excessive Damages					19	G	-0.071	-0.149	-0.153	-0.184		0.0500	1.6280	-6.6000	1.7E+04	1.1E+05		2.9E+03	3721	
18L	J	2	0	3	2	0	0	5	1	G	-0.002	N/A	-0.275	-0.028	0.070	N/A	-0.1690	-0.0004		6.5E+06		4.5E+05		
18R	J	0	2	4	11	2	0	17	7	G	-0.113	N/A	-0.1	-0.048		N/A	0.0350	-0.0410		3.4E+04		7.1E+04		
20L	J	3	4	5	1	0	0	6	1	M	-0.057	-0.06	-0.003	-0.036	0.000	0.0001	-0.0010	-0.0010		6.5E+05		4.9E+05		
20R	J	1	2	2	4	0	0	6	1	G	-0.074	-0.061	-0.104	-0.098		0.0001	-0.0001	-0.0008		6.7E+05		6.4E+05	2697	
22L	J	7	4	4	3	0	0	7	3.5	G	-0.332	-0.149	-0.299	-0.283	0.010	0.0001	-0.9760	0.1000		1.0E+06		2.3E+04	3652	596
22R	J	1	0	0	15	0	0	15	2.2	G	-0.324	-0.131	-0.342	-0.180		0.0100	0.0850	-0.0500		1.2E+06		2.2E+05		
26FL	JUV	1	1	0	8	0	0	8	19	G	-0.275	-0.33	-0.237	-0.256	0.150	0.2370	0.8760	-0.0001		4.6E+03		3.9E+04	2374	
26FR	JUV	0	2	0	7	0	0	7	13	P	-0.087	-0.148	-0.128	-0.152		0.0300	0.0001	0.0002		6.3E+04		8.3E+05		1023
26RL	JUV	3	0	1	4	0	0	5	16	G	-0.119	-0.75	-0.21	-0.245		0.3470	1.6500	0.3500		3.8E+04		4.6E+04		
26RR	JUV	0	3	1	5	0	0	6	33	P	-0.099	-0.07	-0.183	-0.103		0.1580	-0.0010	-0.0002		2.6E+04		9.9E+05		
27FL	JUV	1	3	0	26	0	0	26	10	M	-0.163	-0.193	-0.065	-0.190	0.000	0.2400	0.4760	0.0005	6.7E+05	8.3E+04		6.6E+04		
27FR	JUV	1	0	0	1	0	0	1	4	P	-0.147	-0.267	-0.268	-0.283		0.3200	0.0010	0.0003	1.0E+04	4.9E+05		5.6E+05		
27RL	JUV	0	1	1	3	0	0	4	13	P	-0.077	-0.182	-0.242	-0.272		0.0400	0.3660	0.0720	1.1E+08	1.1E+06		1.1E+05		
27RR	JUV	0	0	0	0	0	0	0	0	P	-0.058	-0.113	-0.235	-0.055		0.0100	0.0010	0.0001	3.4E+06	1.2E+07		9.3E+06		
34L	A	1	0	0	1	1	0	2	1	M	-0.069	-0.042	-0.256	-0.158	0.000	0.0001	0.0010	-0.0007	1.5E+06	7.6E+06		1.3E+07	2693	955
34R	A	1	0	1	2	0	0	3	1	M	-0.062	-0.02	-0.1	-0.178		0.0001	0.0001	-0.0007	8.6E+06	3.3E+07		1.4E+06		
37L	A	0	0	0	5	0	0	5	5	M	-0.062	N/A	-0.104	-0.052	0.020	N/A	0.0040	-0.0003		2.1E+07		3.2E+06		
37R	A	0	0	0	1	1	0	2	3	G	-0.084	N/A	-0.024	-0.058		N/A	0.0001	-0.0002		6.4E+07		8.5E+06		
39L	A	0	0	2	9	0	0	11	3	M	-0.063	-0.122	-0.081	-0.072	0.000	0.0100	0.0001	-0.0003		1.2E+06		4.5E+06		
39R	A	1	0	1	5	0	0	6	2	M	-0.069	-0.087	-0.229	-0.148		0.0001	0.0001	-0.0001		2.9E+06		3.0E+06	2350	
45L	D	3	3	4	0	0	0	4	9	G	-0.12	-0.094	-0.345	-0.164	0.040	0.0200	0.5280	-0.0002		3.4E+05		1.1E+05	2756	
45R	D	2	0	0	0	0	0	0	0	M	-0.082	-0.002	-0.018	-0.026		0.0001	0.0001	-0.0001		2.8E+08		1.3E+06		
46L	D	0	0	1	1	0	0	2	1	G	-0.069	-0.068	-0.048	-0.135	0.190	0.0001	0.0001	-0.0010		6.3E+06		7.7E+06	2581	
46R	D	1	2	2	0	0	0	2	7	G	-0.124	-0.093	-0.121	-0.165		0.1400	0.0010	-0.2700		2.0E+04		4.8E+04		
47L	D	0	1	0	9	1	1	11	3.5	G	-0.092	-0.179	-0.072	-0.154	0.000	0.0300	0.0001	-0.0007		1.7E+06		3.7E+05		
47R	D	3	3	1	9	0	0	10	0	G	-0.071	-0.051	-0.033	-0.090		0.0001	0.0001	-0.0010		2.0E+07		7.8E+05	2568	
50L	D	0	0	1	0	0	0	1	0	M	-0.044	-0.039	-0.047	-0.220	0.000	0.0001	0.0001	-0.0020	2.0E+05	6.2E+07		2.2E+06		789
50R	D	3	7	6	0	0	0	6	5	G	-0.075	-0.187	-0.098	-0.124		0.5800	-0.0020	-0.0010	2.1E+07	3.8E+04		3.6E+05	2721	
54L	T	6	31	52	16	0	0	68	80	Z	-0.129	-0.027	-0.099	-0.144	1.900	0.3800	1.0310	2.3000	5.1E+03	2.5E+04		9.4E+03	3011	
54R	T	3	23	46	7	0	0	53	85	Z	-0.099	-0.026	-0.028	-0.098		0.4600	0.8790	0.9800	3.1E+03	1.3E+04		8.9E+03		
61L	T	14	26	Excessive Damages					100	Z	N/A	-0.179	-0.263	-0.244	N/A?	0.6870	0.0001	30.1000		2.5E+03		1.2E+03	3561	
61R	T	3	75	Excessive Damages					99	Z	N/A	-0.156	N/A	-0.164		3.2300	N/A	10.2000		1.4E+03		1.1E+03		164
62L	T	8	24	46	25	0	0	71	98.5	Z	-0.145	-0.129	-0.163	-0.162	14.800	0.5300	3.3000	-2.3000		1.4E+04		6.6E+03	3012	529
62R	T	5	31	37	23	0	0	60	87	Z	-0.183	-0.133	-0.195	-0.150		1.8100	14.2300	-1.1000		7.5E+03		6.2E+03		
67L	U	0	0	1	0	0	0	1	0.5	M	-0.01	-0.065	-0.012	-0.016	0.000	0.0001	0.0001	-0.0005		1.6E+07		4.1E+05		
67R	U	0	0	1	1	0	0	2	0.5	P	-0.026	-0.121	-0.095	-0.118		0.0001	0.0001	-0.0003		4.3E+06		1.9E+06		
69L	U	0	0	0	0	0	0	0	0	P	-0.129	-0.078	-0.109	-0.126	4.150	0.0001	-0.0010	-0.0310	1.6E+07	3.6E+06		5.2E+06		
69R	U	0	4	4	1	0	0	5	9	M	-0.096	-0.109	-0.156	-0.253		0.1100	0.9350	-0.0080	7.6E+03	1.1E+04		2.0E+04		
74L	U	1	0	0	0	0	0	0	0	M	-0.001	-0.01	-0.006	-0.015	0.000	0.0001	0.0001	-0.0008		1.3E+08		1.1E+06		
74R	U	0	0	2	0	0	0	2	0.1	M	-0.005	-0.061	-0.03	-0.012		0.0001	0.0001	-0.0002		1.2E+07		2.5E+05		
75L	U	0	0	0	1	0	0	1	0.5	G	-0.052	-0.038	-0.064	N/A?	0.000	0.0001	0.0001	0.0001		9.5E+07		3.9E+05		557
75R	U	1	0	0	1	0	0	1	0.5	M	-0.001	-0.144	-0.132	-0.317		0.0100	0.0001	-13.2000		9.9E+05		8.8E+05	3859	
76L	U	0	0	0	0	0	0	0	0	P	-0.027	-0.063	-0.073	-0.090	0.000	0.0001	0.0001	-0.0002		1.1E+06		1.1E+05		
76R	U	0	0	0	5	0	0	5	0.5	M	-0.065	-0.063	-0.004	-0.051		0.0001	0.0001	-0.0002		1.1E+06		1.2E+06		

*Knife adhesion: G (Good), M (Moderate), P (Poor), and Z (Zero testable area). ** N/A: Not Available. ***N/A? indicates uncertainty in data.

Table 3: Listing of crack length above the ECR in each slab.

	Crack Length, in. (Salt Water Ponded Slabs)					
Source	Slab ID	L (12/97)	L (11/99)	R(12/97)	R (11/99)	Note
N	5	3	3	9	14	
N	7	10	14	14	14	
J	16	2	7	10	14	
A	29	6	8	5	5	
A	31	9	12	5	14	Left bar crack severe.
A	36	4	4	0	0	
A	40	0	3.5	3	14	
D	41	0	14	7	14	
D	43	8	8	3	14	
D	48	12	12	7	7	
D	52	0	11	11.5	14	
T	53	3	11	4	12	
T	63	0	4.5	14	14	Severe crack w/ rust stains.
U	66	4	4	4	6	
U	68	2	6	10	10	
U	71	3	8.5	0	9.5	
U	73	13	14	3	3	
	Average	4.6	8.5	6.4	10.5	

	Crack Length, in. (Natural Weathering Slabs)					
Source	Slab ID	L (12/97)	L (11/99)	R (12/97)	R (11/99)	Note
N	3	1	1	1	1	
N	6	6	6	5	14	Right side crack severe.
N	8	2	2	14	14	
N	9	4	4	2	2	
N	11	6	6	5	5	
JUV	12	10.5	10.5	13	13	
J	15	11	14	0	0	
J	18	8	8	8	8	
J	20	3	14	7	7	Left side crack severe.
J	22	4	4	1	1	
JUV	26	4	4	10	10	
JUV	27	13	14	4	4	Transverse crack across entire width.
A	34	11	11	10	10	
A	37	6	6	4	14	
A	39	3	3	3	3	
D	45	11	11	8	8	
D	46	3	3	14	14	
D	47	2.5	2.5	3	3	
D	50	7	7	4	4	
T	54	0	14	0	14	Cracks on both sides severe.
T	61	6	6	12	12	
T	62	2	2	14	14	
U	67	2.5	2.5	11.5	11.5	
U	74	11	11	7	7	
U	75	5	5	8	8	
U	76	5	5	14	14	Right side crack severe.
	Average	5.5	6.5	6.8	8.0	

Figure 1 presents a plot of crack length above individual ECRs that remained for the final autopsy versus macrocell current with each bar source identified. No dependence is apparent between crack length and either macrocell current or bar source. The same result was obtained for the natural weathered slabs. This supports the conclusion that the cracking source was other than corrosion related.

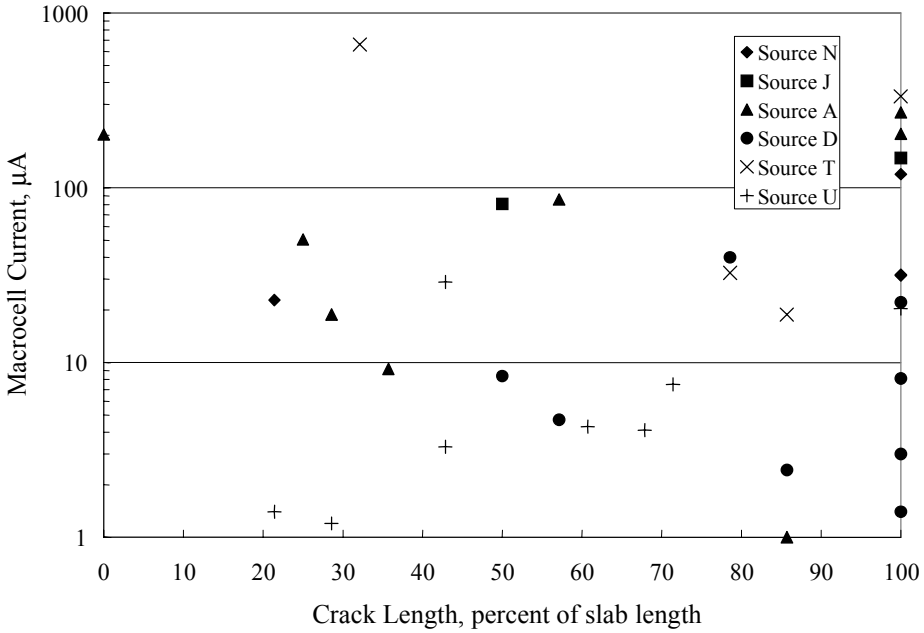

Figure 1: Plot of macrocell current versus crack length as of November, 1999.

Condition of the ECRs subsequent to the exposure varied from poor to excellent, as illustrated by the photographs in Figures 2-4. The right bar from slab 63 (source **T**), which is shown in Figure 2, exemplifies the former behavior (poor), where corrosion products were apparent over much of the bar upon its removal from the slab ("before" condition); and the coating was entirely disbonded such that it could be readily removed using a knife ("after" condition). This revealed that the complete steel surface was corroded. Figure 3 illustrates the appearance of intermediate behavior (right ECR from slab 6 (source **N**)) in that for this example the coating was only partially disbonded and rust was apparent at local regions only. The marker dots on the bar in the "before" photograph identify sites where holidays were detected. Note that the disbonded regions correspond to these holiday locations on virtually a one-to-one basis. Lastly, Figure 4 shows the appearance of the left ECR from slab 66 (source **U**) that was found to

(a)

(b)

Figure 2: Photograph of the top of the right ECR from slab 63 (a) before removal of disbonded coating and (b) after removal.

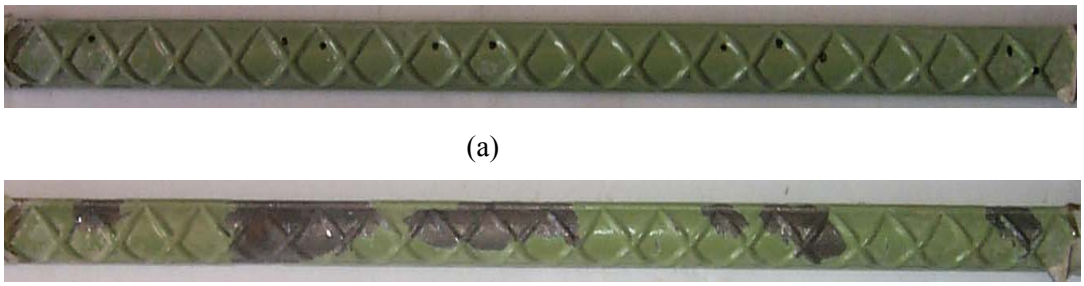

(a)

(b)

Figure 3: Photograph of the top of the right ECR from slab 6 (a) before removal of disbonded coating and (b) after removal.

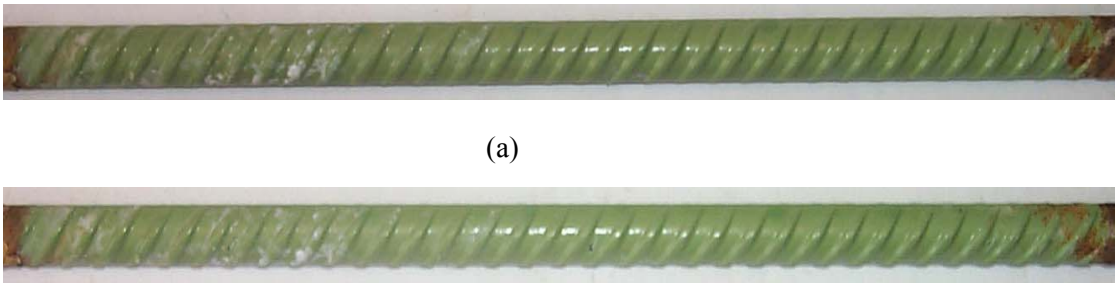

(a)

(b)

Figure 4: Photograph of the top of the left ECR from slab 66 (a) before removal of disbonded coating and (b) after removal.

be in excellent condition. This specimen had few holidays, and the coating remained bonded. Greater disbondment, often accompanied by anodic blisters, was generally apparent on the underside of the bars, suggesting that macrocell action in conjunction with the bottom bar was a factor.

CHLORIDE CONCENTRATION

Figure 5 shows the values for chloride concentration that were measured at the trace of both top and bottom bars at the time of the third and fourth autopsies (see also Tables 1 and 2). These data indicate that there was little difference between the chloride concentration at the two times for the natural weathering (NW) slabs, as should be expected; but the salt water ponding (SWP) resulted in an increase by approximately a factor of five. The cracks above the ECR trace on many of the specimens undoubtedly contributed to this. The data also show that chlorides had migrated into the bottom portion of the slabs, which were cast without admixed chlorides, and had reached levels in excess of the chloride threshold (250-500 ppm) in most cases.

COATING DEFECTS

Four types of defects were found upon the autopsied ECR: 1) mechanical damage, including mashed spots, 2) blisters, 3) coating cracks, and 4) pin-holes. In most cases, the number of defects upon autopsy was greater than detected initially, indicating that additional defects occurred either during slab fabrication or upon exposure (or both). The fact that defects formed during the hot water and ambient temperature aqueous solution exposures of these same bars (9)

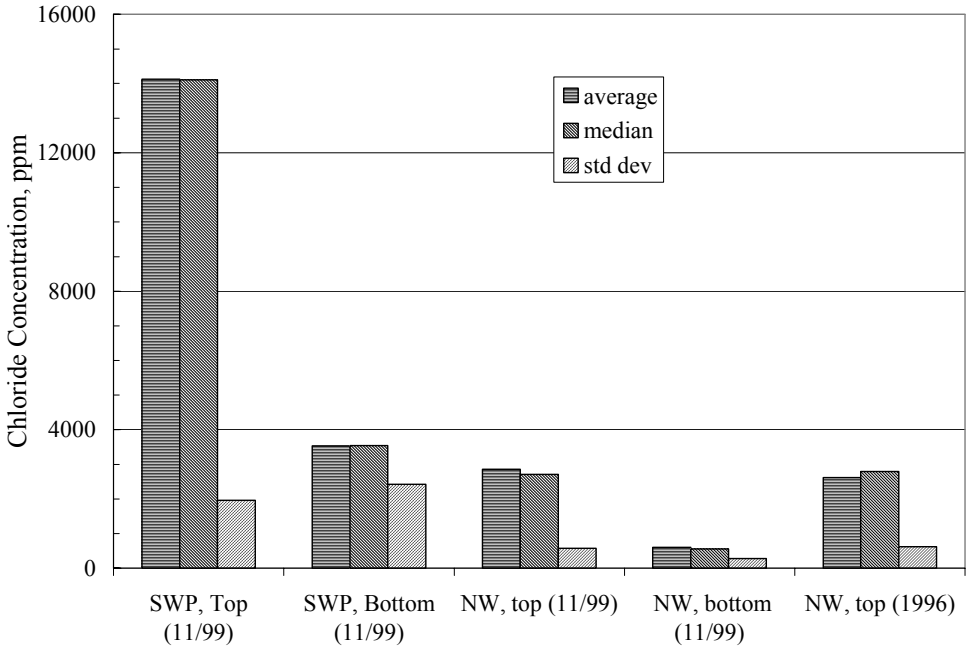

Figure 5: Chloride concentration at the top and bottom bar depths at the time of the third and fourth autopsies.

suggests that at least some defects developed during the exposure. Figure 6 shows an example of coating cracks and Figure 7 of an anodic blister, both before and after stripping away the coating. This removal of the coating revealed a pit and corrosion products. Figure 8 shows a second example of an anodic blister after coating removal along with the back side of the coating. Invariably, such pits were relatively deep and located on the underside of the bar, indicating that they occurred in conjunction with macrocell action. Coating cracks and bare areas were the predominant types of defect, as shown by Figure 9. It was consistently observed through the autopsies that fine cracks were the primary coating defect type that resulted as deterioration

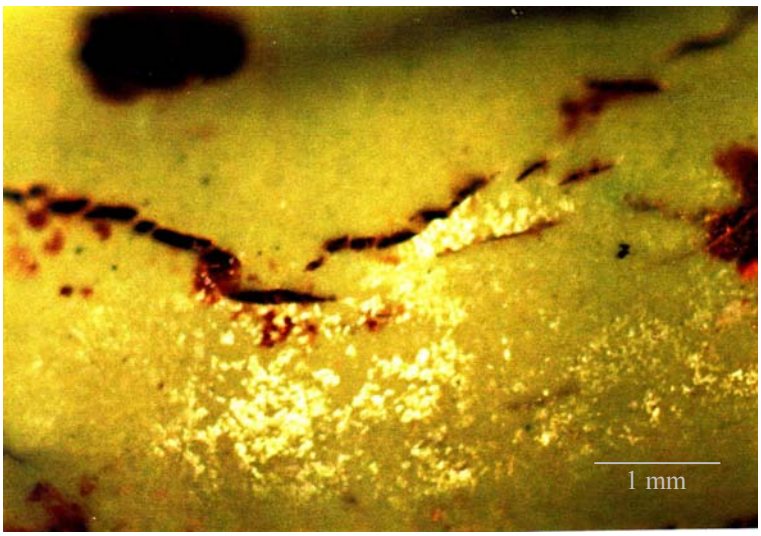

Figure 6: Photograph of coating cracks on Left Bar of Specimens 17.

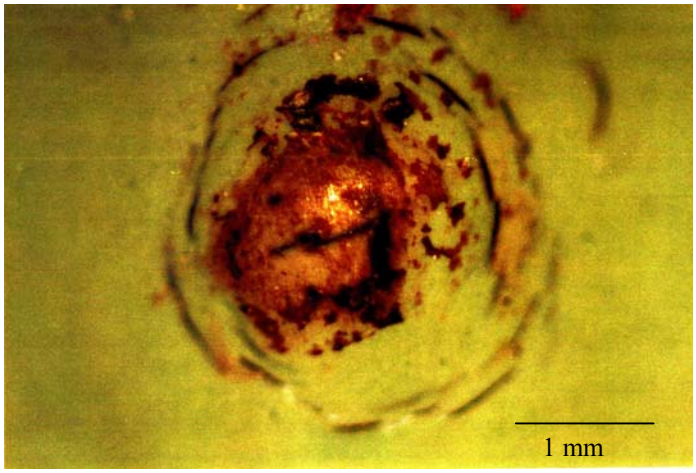

(a)

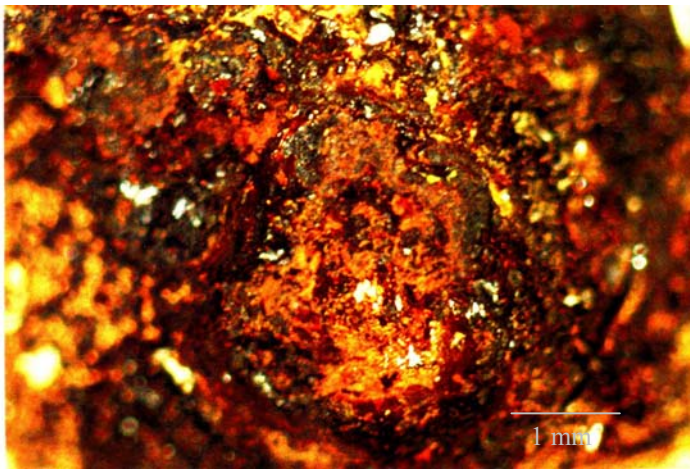

(b)

Figure 7: Photograph of a coating blister on a bar from specimen 17 prior to (a) and after (b) coating removal.

progressed and the coating became brittle. Also, while the percentages of bare areas and coating cracks were comparable for the NW exposed specimens (46 versus 52 percent, respectively), these percentages were 22 and 74 (bare areas and coating cracks, respectively) for the SWP exposure, which is indicative of greater tendency for the latter to form under this exposure condition (SWP) compared to the former. Also, although the percentage of pin holes (holidays) was relatively low for both exposures, this defect type developed to a greater extent on bars with cross deformations and on bars for which the coating was relatively thin. However, the average coating thickness was within specification in all cases, as noted above.

Figure 10 plots the number of initial defects versus the number of final ones for bars that were analyzed during the fourth autopsy with the data being partitioned according to the type of exposure (natural weathering versus salt water ponding). Cases of no initial defects are represented as 0.1. In instances where the final number of defects was excessive, due to coating cracks in most cases, a value of 100 was assigned. If no defects developed for a particular bar subsequent to the initial count, then the corresponding datum lies along the sloping line. The fact that most data are above this line indicates that additional defects formed in the great majority of

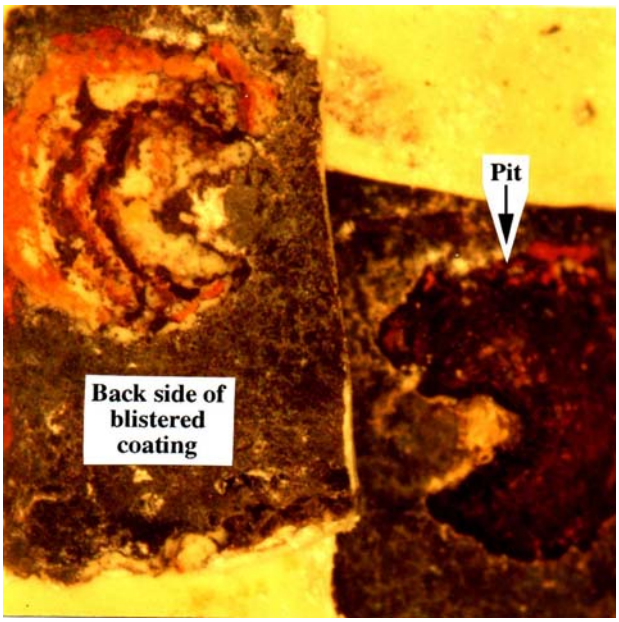

Figure 8: Photograph of a pit beneath a coating blister and the and back side of the coating as viewed upon a bar from specimen 64.

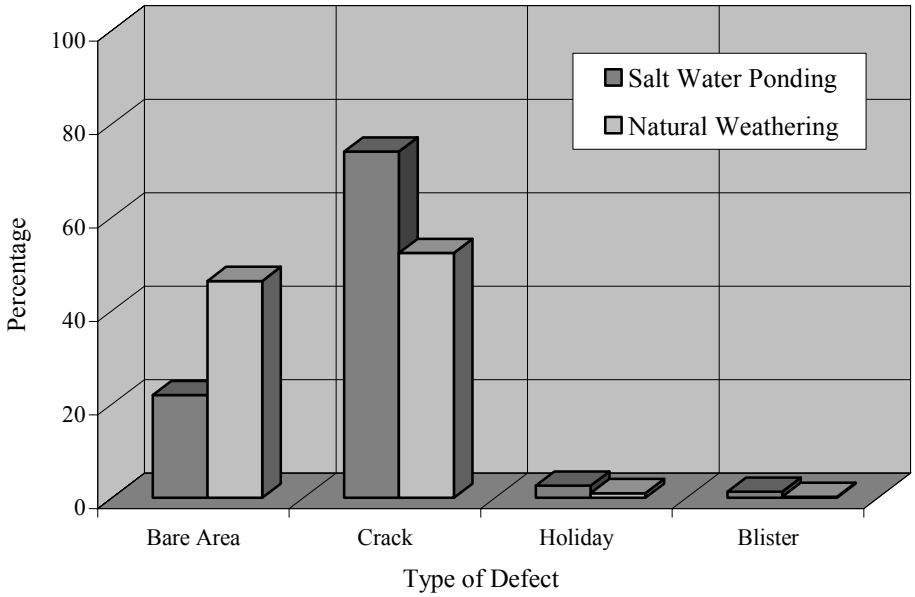

Figure 9: Percentage of each defect type for the two exposures.

cases. In some instances, this increase was by more than an order of magnitude and was greater for the more severe exposure (salt water ponding compared to natural weathering). The latter observation (greater increase in the number of defects for the salt water ponded specimens) indicates that at least some of the increase was a consequence of exposure as opposed to damage during specimen fabrication. Coating cracks were mainly responsible for this increase, as discussed above. While 16 salt water ponded and 18 naturally exposed bars that had no initial

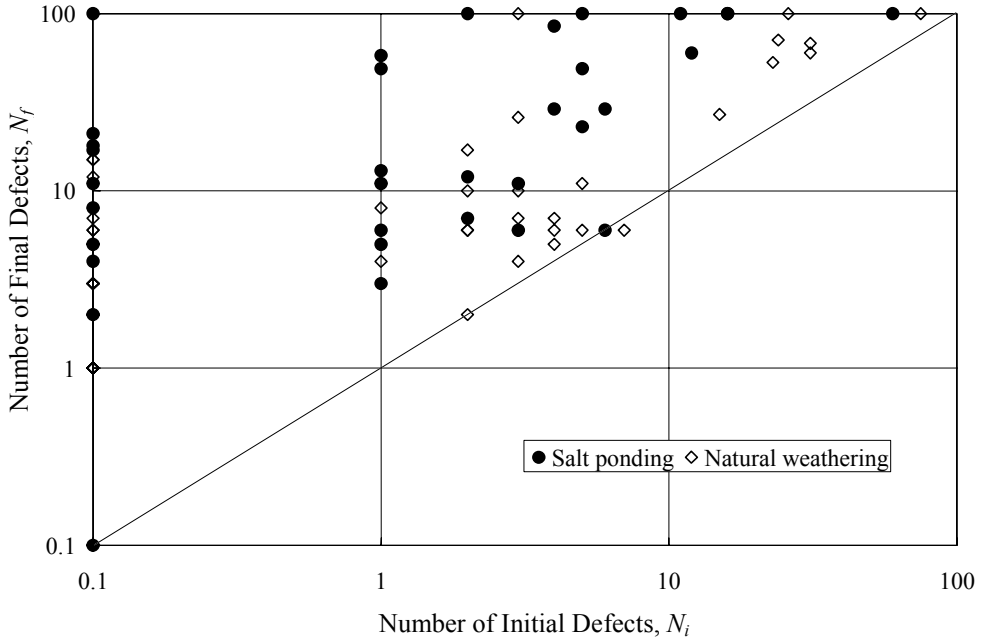

Figure 10: Plot of the initial number of coating defects versus the final number for specimens of the fourth autopsy.

defects developed defects during the exposure, one bar in the former category (salt water ponded) (**68L (U)**) and four in the latter (**27RR*** (**JUV**), **45R** (**D**), **69L** (**U**), and **76L** (**U**)) did not. This indicates that, at least in select cases, ECRs remained defect free for the entire six-plus years. The fact that ECRs from sources **D** and **U** performed well in accelerated tests such as DW/HWT (distilled water/hot water test) and Solvent Extraction Weight Loss is consistent with this (see Table A1).

Figure 11 replots data for the natural exposure specimens in Figure 10 but with each bar identified according to source. Results from the third autopsy (1996) are included also; and it is apparent that the number of coating defects approximately doubled between these two times (1996 and 1999). Also, while more additional coating defects formed for bars with a high number of initial defects compared to bars with few, Table 4 indicates that the ratio of these two (number of final defects to the number of initial) was roughly constant. In developing the data in Table 4, specimens with excessive coating defects were not included.

Correspondingly, Figure 12 shows a plot similar to the one in Figure 11 but for the salt water ponded exposure specimens. Assuming that a power law expression adequately represents the data, although the fit is not as good as in Figure 11, and recognizing that the slope of this best fit line is near unity, then the number of final defects exceeded the initial by a factor of approximately seven. On this basis, the number of defects that developed during the 13 months of salt water ponding was almost twice what occurred during six years of natural weather/potable water ponding exposure. Table 5 tabulates the ratio of final-to-initial defect numbers according to bar source and shows that on average a seven fold increase in the number of defects occurred for these specimens. Presumably, the difference for these, compared to the fourth autopsy NW

* The two letter designation pertains to ECRs that had undergone prior UV exposure where, as explained in Appendix A, each bar was comprised of two sections.

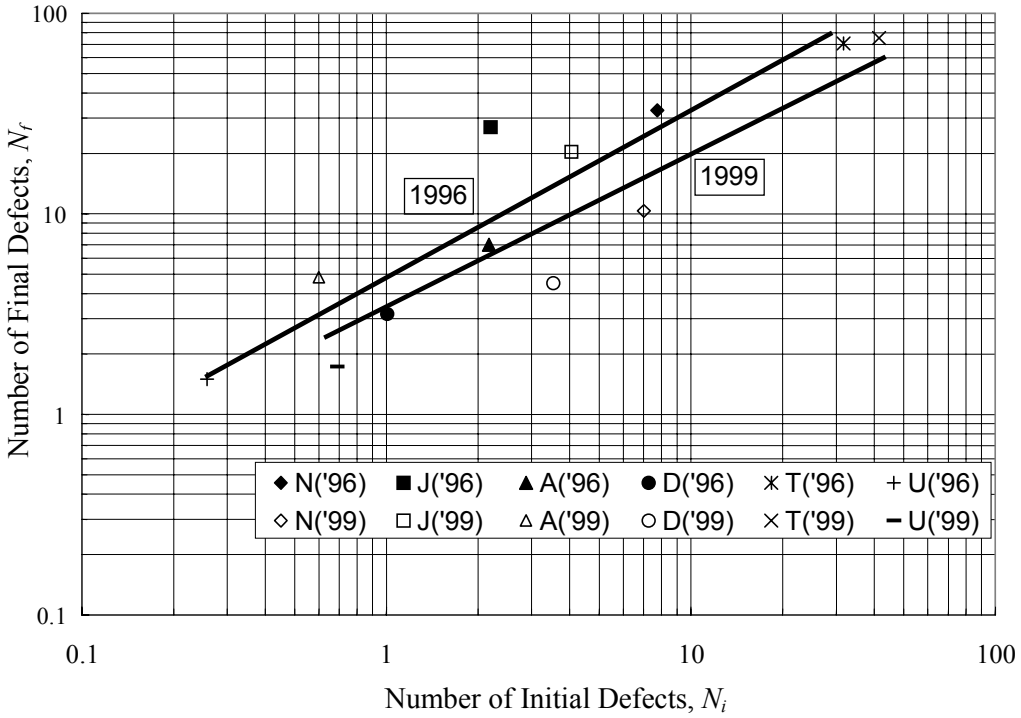

Figure 11: Replot of the natural weather exposure data from Figure 10 (1999 autopsy) along with results from the 1996 autopsy with data for each bar source averaged.

Table 4: Comparison of the ratio of average final-to-initial number of defects for the third and fourth autopsy natural weathered specimens according to bar source.

Source / Category	Ratio of Final -to-Initial Number of Defects, N_f/N_i						Overall Ratio
	N	**J**	**A**	**D**	**T**	**U**	
2nd and 3rd Autopsy ECRs	1.1	7.8	3.2	3.2	2.4	1.5	3.2
4th Autopsy ECRs	1.5	3.4	8.1	1.3	1.9	2.5	3.1

specimens, was the more severe exposure condition during the final 13 months. As for Table 4, only data for bars that did not have excessive coating defects were included.

The data in Figures 11 and 12 indicate that **U** source bars were one of the, top performers, if not the top performer, with regard to number of defects. As noted earlier, these bars were chromate conversion coated. While this surface treatment may have been responsible for the lesser number of coating defects, there is no way of confirming this.

Figure 13 presents a plot of defect ratio versus time based upon the data in Tables 4 and 5. The NW data (Table 4) suggest that the number of coating defects increased initially during the exposure but subsequently became constant. However, this is tempered by the fact that N_i for the third autopsy specimens averaged 16 percent higher than for the fourth autopsy ones. Consequently, it was assumed in constructing Figure 13 that defects developed at a rate that was constant with time. On this basis, the rate of defect development for the NW exposed bars

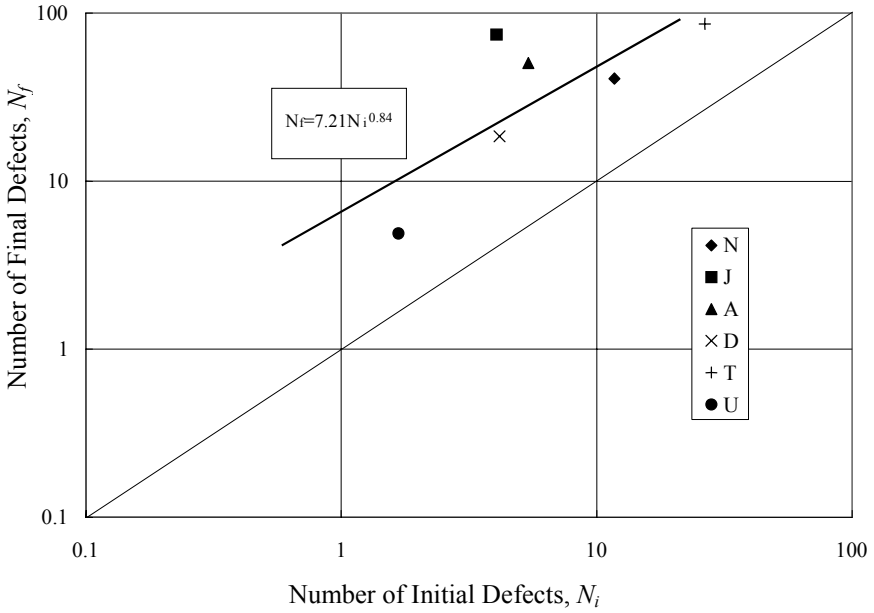

Figure 12: Plot of the number of final defects versus the initial number for salt water ponded specimens (1999 autopsy) with the data averaged according to bar source.

Table 5: Comparison of the ratio of average final-to-initial number of defects for the salt water ponded specimens according to bar source.

Source / Category	Ratio of Final -to-Initial Number of Defects						Overall Ratio
	N	**J**	**A**	**D**	**T**	**U**	
4th Autopsy ECRs	3.5	18.4	9.4	4.4	3.3	2.9	7.0

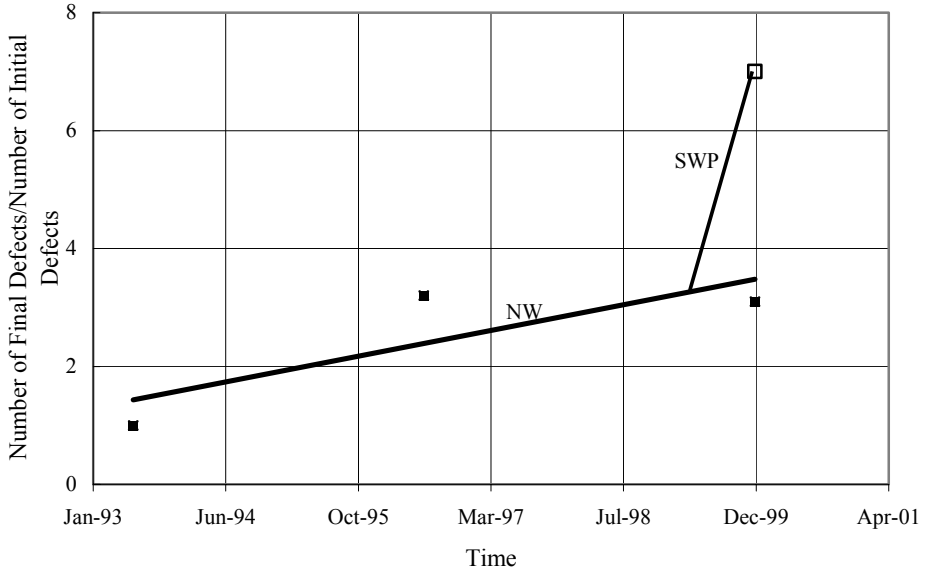

Figure 13: Plot of N_f/N_i versus time based upon the data in Tables 4 and 5.

conforms to the expression,

$$\frac{N_f}{N_i} = 0.40 \cdot T + 1, \quad (1)$$

and for the SWP specimens,

$$\frac{N_f}{N_i} = 2.67 \cdot T + 1, \quad (2)$$

where T is the exposure time in years.

CORROSION POTENTIAL AND MACROCELL CURRENT

Epoxy-coated bars that exhibited a relatively low macrocell current and positive potential generally showed minimal corrosion and vise versa, as determined visually when the slabs were broken apart. Figure 14 shows corrosion potential for individual bars at select times during the exposure with the data partitioned according to natural weathering versus salt water ponding. The two curves are plotted according to the average potential at each time. Thus, there was relatively little change in potential with time for the natural weather exposed specimens, whereas a negative potential shift of 450 mV resulted from the 13 months of salt water ponding. This suggests a much more active corrosion state for the latter compared to the former.

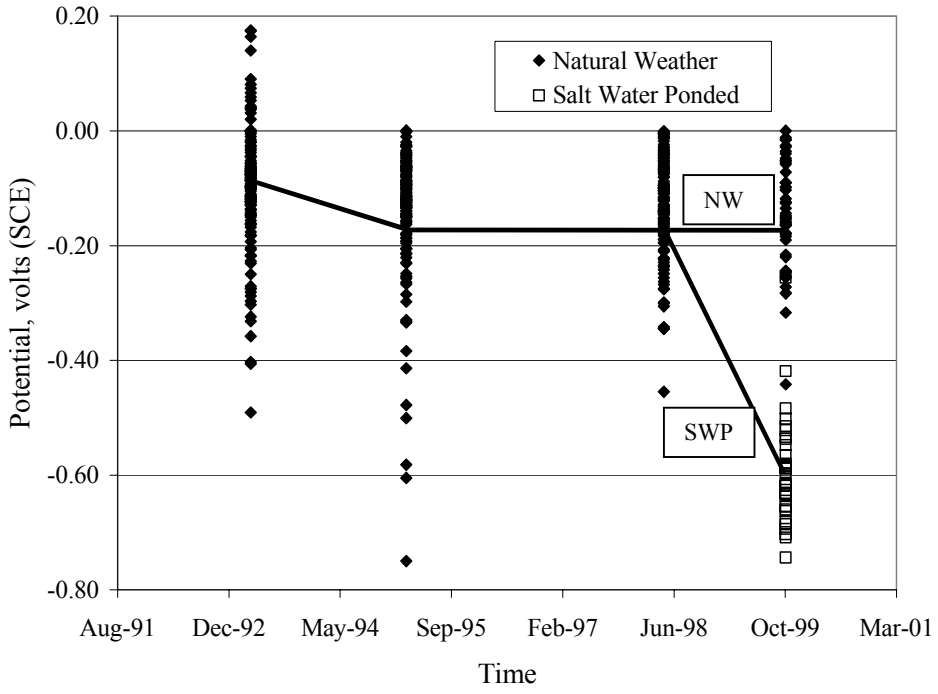

Figure 14: Open circuit potential data for the test slabs at select times during the exposure.

Likewise, Figure 15 plots potential versus macrocell current for all specimens that remained for the final autopsy. This shows a general relationship where current increased with decreasing

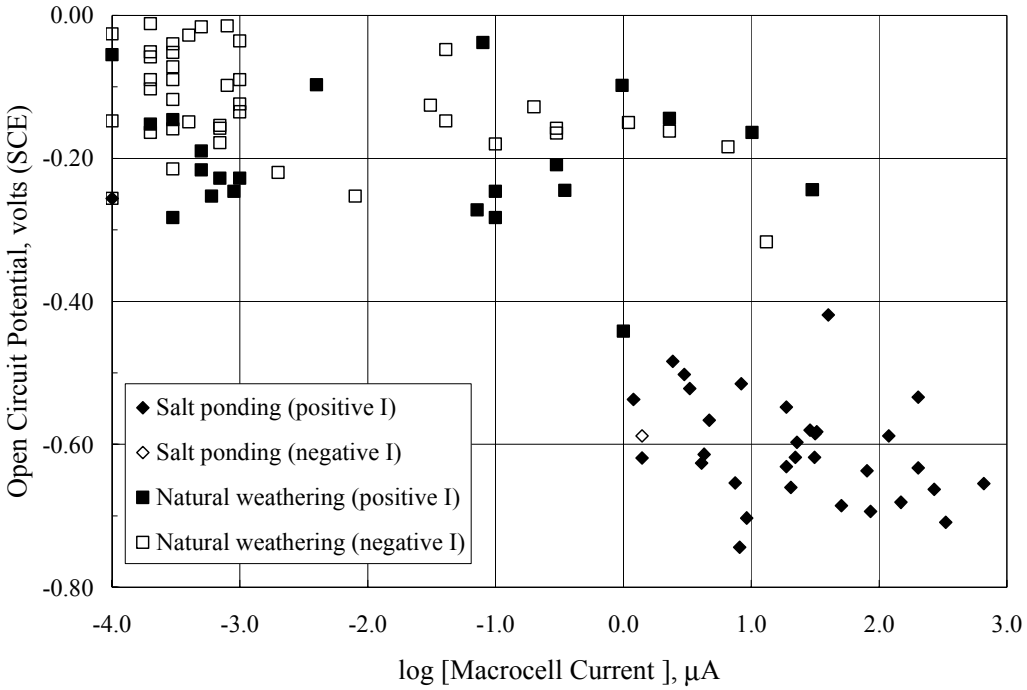

Figure 15: Plot of macrocell current versus open circuit potential for slabs just prior to the final autopsy.

(more negative) potential with the natural weathering specimens occupying the low current, relatively positive potential regime and the salt water ponded ones the high current, negative potential regime. Some currents were negative, particularly for the natural weathering specimens, indicating that the bottom black steel was anodic to the upper mat ECR. However, in the majority of cases where this occurred, potential was positive to the threshold value below which atmospherically exposed steel in concrete is considered to be active (OCP was positive to –0.28 volts (SCE)), suggesting that both steel mats were passive. Chloride intrusion into the bottom mat, as noted above, combined with protective action of the epoxy coating is thought to have been responsible for this. Table 6 shows that the percentage of ECRs that exhibited such a current reversal increased with exposure time. Consistent with this, bars with negative currents typically had relative few coating defects (bars from sources **U**, **D**, and **A**).

Table 6: Percentage of natural weathering specimens with current reversal at different times.

Date of Data Acquisition	Percentage of ECRs with Current Reversal
April, 1993	0
March, 1995	0
June, 1996	16
May, 1998	14
November, 1999	64

As discussed above, hairline cracks developed on the upper concrete surface along the trace of almost all ECRs during the course of the exposures; and these grew with time. These cracks

were attributed to subsidence and not corrosion. In this regard, Table 7 presents data for the two ECRs that did not exhibit any concrete cracking at the time of the final autopsy. These results and comparison of these with data from other bars in Figure 10 indicate that the bars without associated concrete cracks were not atypical; and no reason is apparent why, from a corrosion standpoint, the concrete above these should be less damaged than for other specimens. Alternatively, the fact that the corrosion state for these two bars is typical of others indicates that presence of the cracks did not accelerate ECR deterioration within the time frame of the exposures.

Table 7: Data acquired at the time of the final autopsy (12/99) for ECRs where concrete was not cracked.

ECR Number	Exposure	Defects	Disbondment, percent	Coating Adhesion	Potential, v (SCE)	Current, μA	*Z*, Ohms
36R	SWP	Excessive	60	Moderate	-0.534	202	790
15R	NW	Excessive	19	Good	-0.184	-6.6	2,900

COATING ADHESION

Adhesion of the coating on the ECRs from the second, third, and fourth autopsies was evaluated qualitatively by cutting and peeling back the coating from a minimum of six sites per bar where the coating remained bonded. Quality of the bond was then classified as either "good", "moderate," "poor," or "zero." Figure 16 shows the results from this. Findings from the second autopsy are not included because of the small number of bars involved. Also, there was no obvious adhesion distinction between the weathered and non-weathered bars from the third autopsy; and so the data for these were grouped together. If it is assumed that the NW and SWP specimens possessed the same coating adhesion distribution prior to the salt water ponding (October, 1998), then these results suggest that the ponding caused some loss of adhesion. However, such an assumption is tempered by the fact that the adhesion distribution for the third

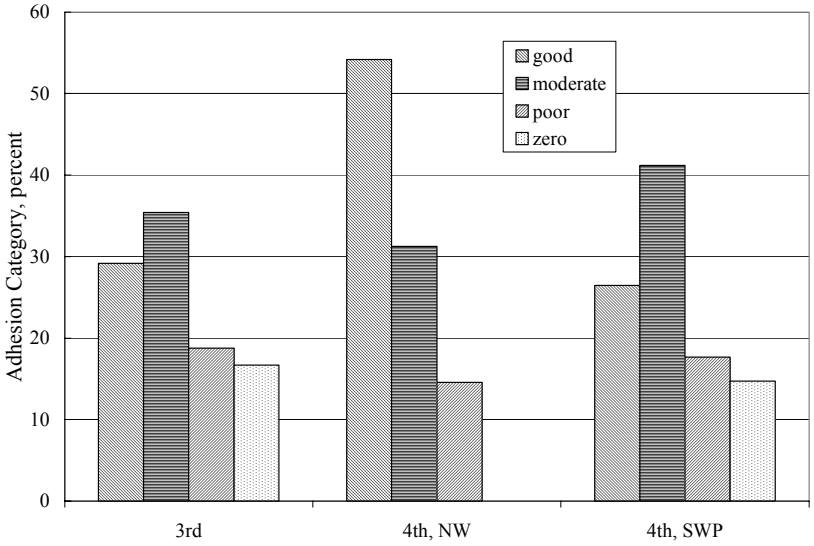

Figure 16: Adhesion of the coating upon ECRs recovered from the third and fourth autopsies.

autopsy specimens is indicative of better adhesion than the fourth autopsy NW ones. In fact, the adhesion distributions for the third autopsy and fourth autopsy SWP specimens are about the same. It is concluded that the salt water ponding did not have a pronounced affect upon adhesion at locations where bonding between the coating and steel was retained. It should be recognized, however, that the knife adhesion testing was performed several days after termination of ponding because of the time required to section and break open the slabs and recover the ECRs. Consequently, any wet adhesion loss that had transpired may have recovered, at least partially, during this period with the test results being affected accordingly.

COATING DISBONDMENT

The extent of coating disbondment was measured for individual ECRs that were recovered from the third and fourth autopsies by using a utility knife to peal back and remove loose coating beginning at coating defects and estimating the percent of the entire bar area that became exposed. Figure 17 plots these data versus macrocell current. Results for bars from the third autopsy (1996 natural weather (NW) exposure) fell into two groups, one at relatively low current (essentially zero to a fraction of a microamp) and one at high (0.1 to 200 μA) with percent disbondment for both sets being independent of current. Data for the SWP specimens tended to be displaced toward higher current for a given percent displacement than for the NW ones. Also, the percent disbondment for the SWP specimens increased with increasing current for percent disbondments in excess of about ten, although the effect is somewhat obscured by the relative scaling of the axes. The cause and affect here is uncertain in that high current may have caused disbondment or vise versa. Also, the percent disbondment was roughly independent of whether ECR current was anodic (positive) or cathodic (negative). A likely explanation for the current-disbondment relationship is that coatings with a high density of defects developed greater disbondment and this, in turn, led to higher current.

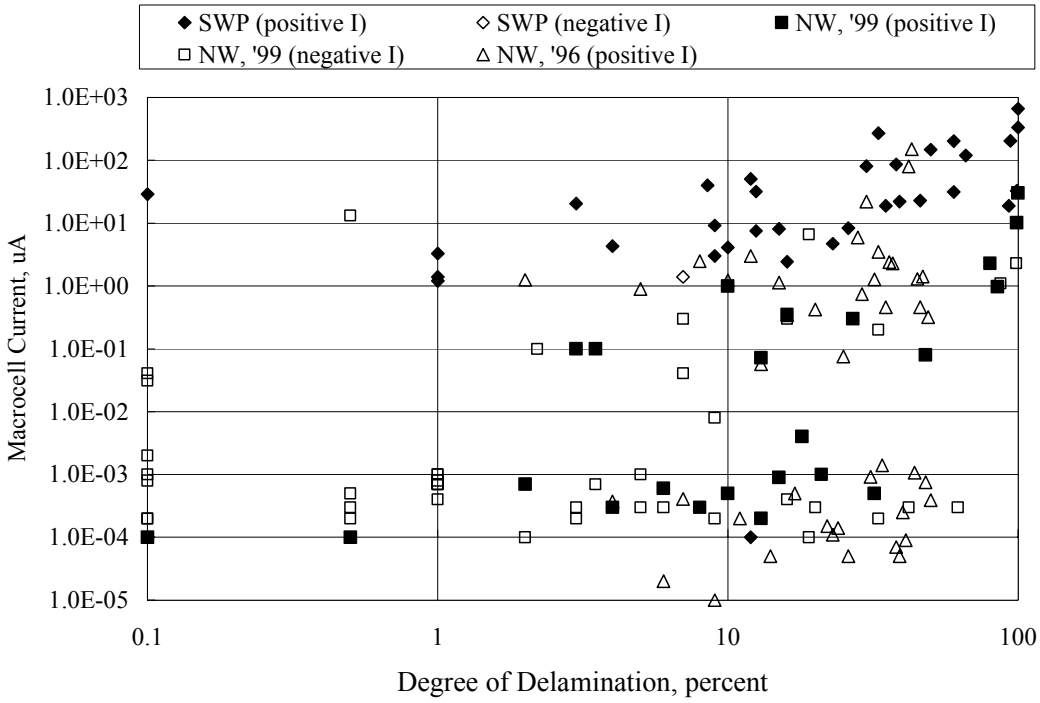

Figure 17: Plot of percent coating disbondment versus macrocell current for ECRs recovered from the third and fourth autopsies.

Correspondingly, Figure 18 plots the percent of coating disbondment versus the number of final defects for the same specimens as in Figure 17. This shows a general trend, albeit with a large amount of scatter, where disbondment was low and independent of the number of final defects when the number of defects was less that about 5-10 but increased with increasing defects above this. Unlike the situation in Figure 17, however, where the NW-1996 and NW-1999 data are partitioned into two regimes, in Figure 18 a common trend applies to all specimens. Figure 19 shows a plot of current versus the number of final defects, again for the third and fourth autopsies, and indicates that macrocell current was independent of the number of defects when the latter parameter was less than about ten but increased sharply for defect numbers above this. The data for both natural weathering specimen groups (1996 and 1999 autopsies) with relatively large numbers of defects was about the same, whereas results for the salt water ponded ones were displaced toward higher current values. This was probably a consequence of a combination of greater potential difference between the two mats and reduced concrete resistivity in the latter case (salt water ponded) compared to the former (natural weathered).

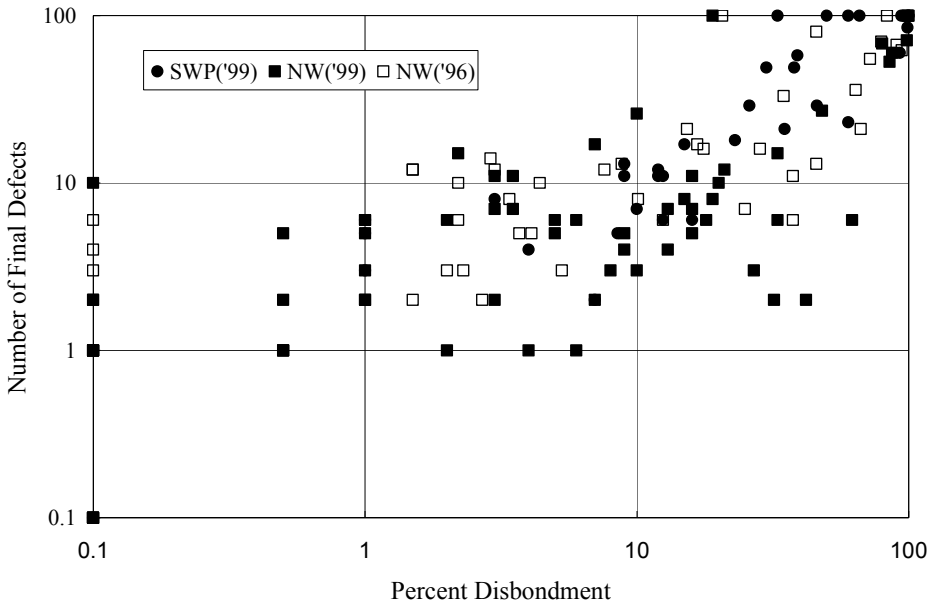

Figure 18: Plot of percent disbondment versus the number of final defects for specimens from the third and fourth autopsies.

A high quality coating with few or no defects is expected to provide a resistive barrier to flow of macrocell current, either to or from ECR. However, local microcell action beneath any disbonded areas of the coating can result in further disbondment. In situation where current is positive (anodic), disbondment results from cathodic processes at or near the front between the intact and disbonded coating (the farthest distance beneath the disbonded coating from the active site (coating defect)). If, on the other hand, the current is negative, then the entire ECR becomes a cathode; and disbondment occurs locally at a rate proportion to the magnitude of this current. This may explain the low macrocell current (either positive or negative) – large coating disbondment data in Figure 17.

IMPEDANCE

A conclusion that was reached from testing performed in NCHRP Project 10-37 was that the

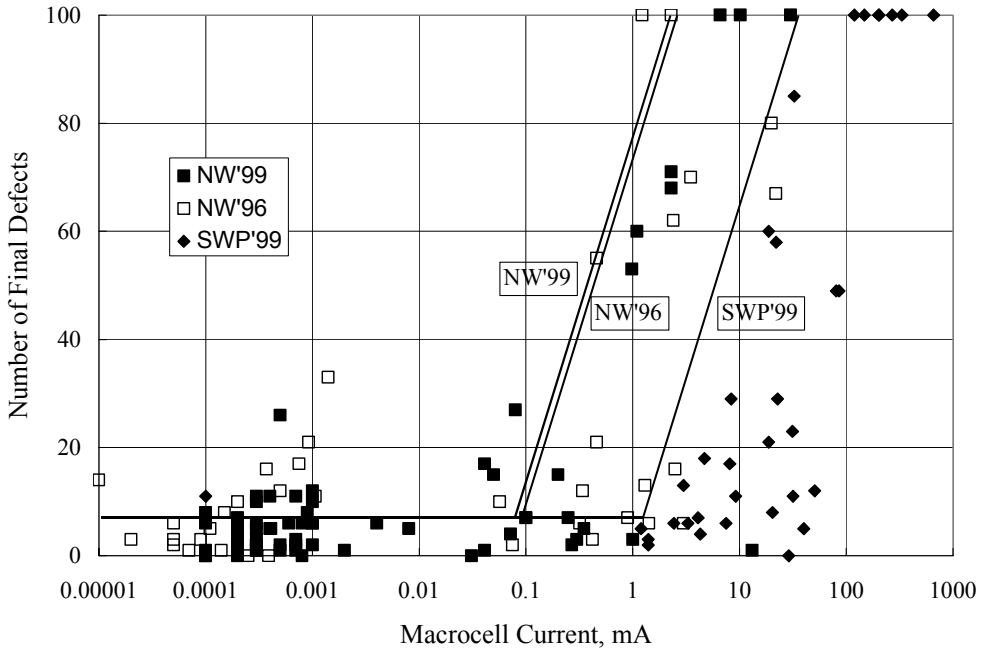

Figure 19: Plot of macrocell current versus the number of final defects for both natural weathered and salt water ponded specimens.

impedance of ECRs at 0.1 Hz. was indicative of the extent to which conductive pathways were present in the coating (greater concentration of conductive pathways corresponded to reduced impedance) (9). Consequently, the modulus of impedance (log /Z/) was measured periodically throughout the present exposure program; and Figure 20 plots data for each individual ECR at different times with the average and median being shown. The data indicate that, first, the change in the average and median impedance for the natural weathered specimens at the different

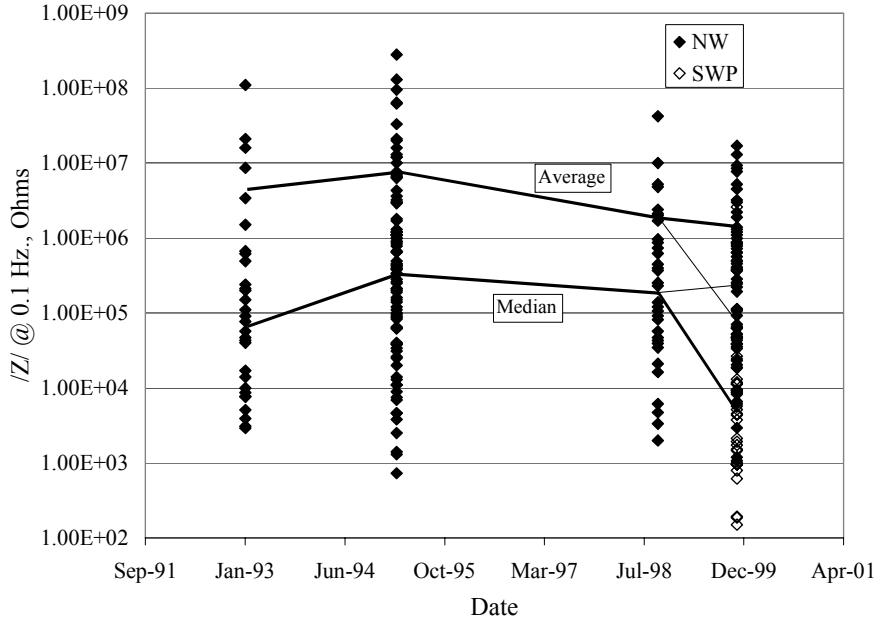

Figure 20: Impedance of individual ECRs at different times during the exposure.

measurement times was by no more than several-fold and, second, the rate of impedance change was small; however, 13 months of salt water ponding reduced the average impedance by more than one order of magnitude and the median by even more. The former trend is similar to the variation in the average OCP with time, as reported in Figure 14.

Impedance for the individual ECRs fluctuated with time, particularly in cases where the magnitude of this parameter was relatively high. The variations were, however, typically within an order of magnitude. Impedance for some bars increased with time, possibly due to buildup of corrosion products at coating defect sites or clogging of coating pores (or both), as discussed previously (9). Figure 21 presents a plot of impedance that was measured for individual ECRs in March, 1995 versus the value at subsequent times before and after salt water ponding. This shows that the NW data are evenly distributed to either side of the one-to-one line and that the 1998 average and the 1998 and 1999 medians fall close to the one-to-one line, indicating that these parameters did not change during the times considered (1995 to either 1998 or 1999). The fact that the average for the NW 1999 specimen data is about an order of magnitude below the one-to-one line probably reflects a relatively large *Z* decrease for a few bars. The SWP data, on the other hand, are all below the one-to-one line with the average and median lying below the corresponding values for the NW specimens by a factor of 20 and 69, respectively. Again, the fact that the average is less than the median in each case reflects an influence from a few bars with relatively high impedance.

Figure 22 plots impedance for specimens that remained at the end of the third and fourth autopsies versus percent coating disbondment. The salt water ponded data are represented here to one percent disbondment by one power law expression, whereas the natural weathered specimens

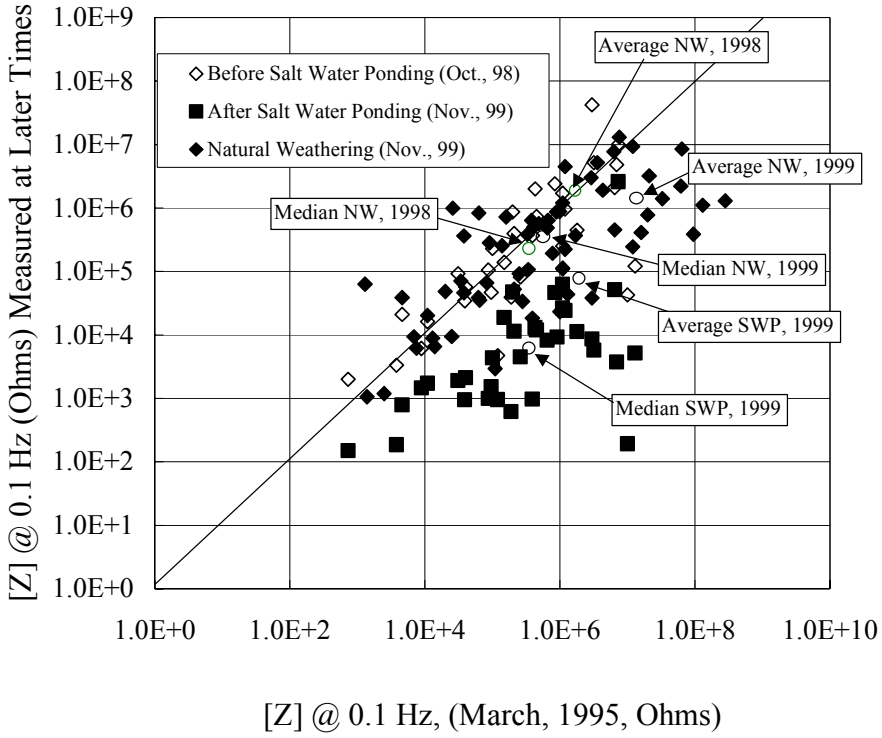

Figure 21: Comparison of impedance of individual ECRs as recorded at different times.

(1996 (preweathered and non-preweathered) and 1999) are represented in terms of a second, albeit in spite of relatively large scatter. This shows that impedance decreased with increasing disbondment such that a one order of magnitude change in one parameter resulted in an order of magnitude change in the second. Also, the 13 months of salt water ponding decreased impedance by approximately one order of magnitude at a particular percent disbondment compared to the natural weather exposure. Alternatively, an order of magnitude greater disbondment was required to affect a given impedance in the NW compared to SWP ECRs. Considering that ten percent disbondment corresponds to approximately ten coating defects per 14 inch specimen length (Figure 18), Figure 22 indicates the corresponding log/*Z*/ for natural weather exposure was about five and for salt water ponding four (specific impedances of 1.8×10^7 and 1.4×10^6 Ωcm^2, respectively).

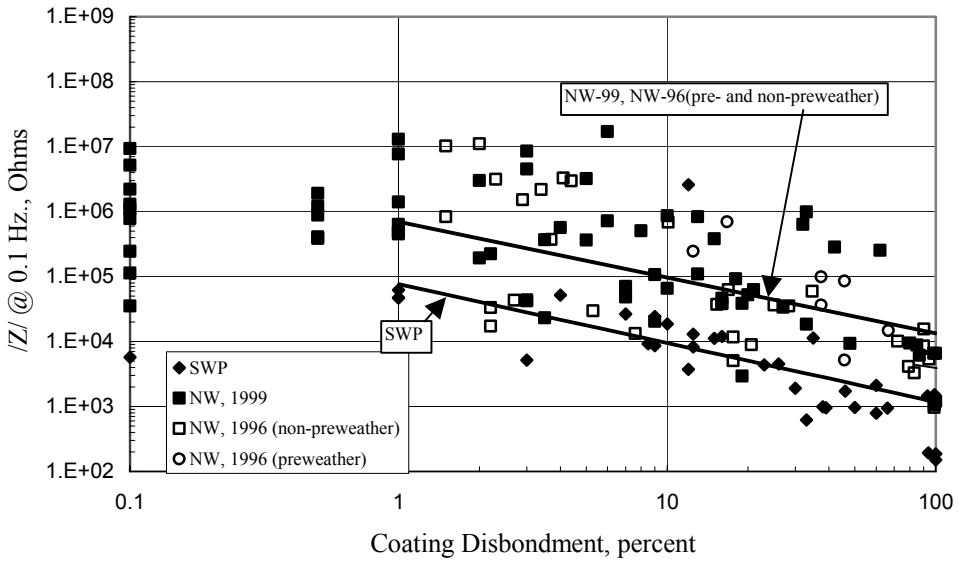

Figure 22: Plot of percent impedance at 0.1 Hz. versus percent coating disbondment.

Figure 23 shows a plot of modulus of impedance @ 0.1 Hz. versus macrocell current for specimens that remained at the final autopsy. Data for that time (November, 1999) as well as an earlier data set (May, 1995) are shown, the latter for comparison purposes. A general correspondence of the two NW data sets is apparent, which is consistent with the finding above that the rate of coating defect development during the time span between these two autopsies was relatively low (Equation 1). The plot indicates that impedance for the NW specimens decreased with increasing macrocell current beyond about 0.01 μA such that an order of magnitude decrease in one parameter resulted in a similar decrease in the other. The same general trend is apparent for the SWP specimens but with the data being displaced toward greater current by approximately one order of magnitude.

Figure 24 plots impedance versus the number of final defects for bars from the third and fourth autopsies. Each of the three sets of data has been fitted by a power law relationship considering only cases of one or more coating defects per bar. These show that both sets of NW data conform to essentially the same trend curve, albeit with a relatively large amount of scatter, whereas results for the SWP exposure are displaced toward lower impedance by about one order of magnitude; that is, a ten-fold greater number of defects was required to affect a particular impedance in the NW compared to SWP exposure. range. Such a projection is consistent with the

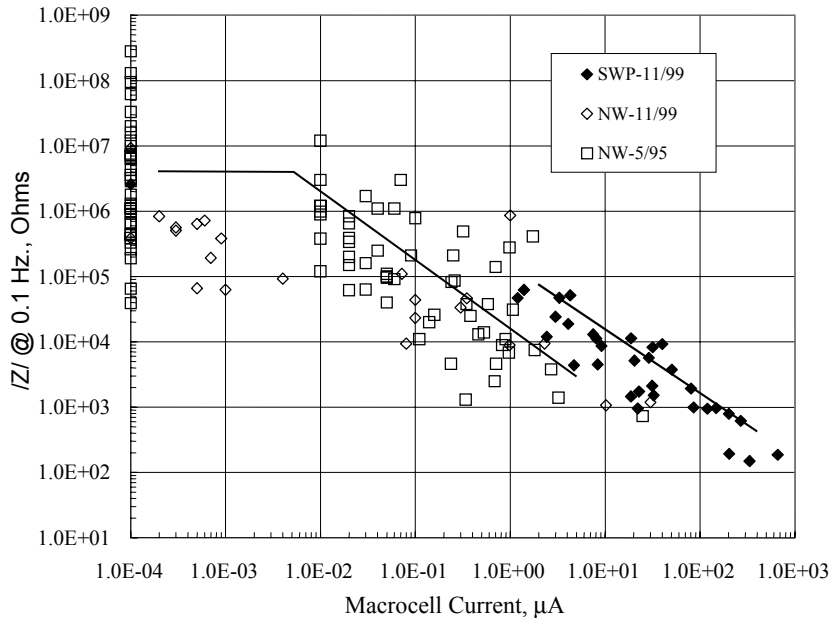

Figure 23: Plot of impedance @ 0.1 Hz versus macrocell current for specimens from the third and fourth autopsies.

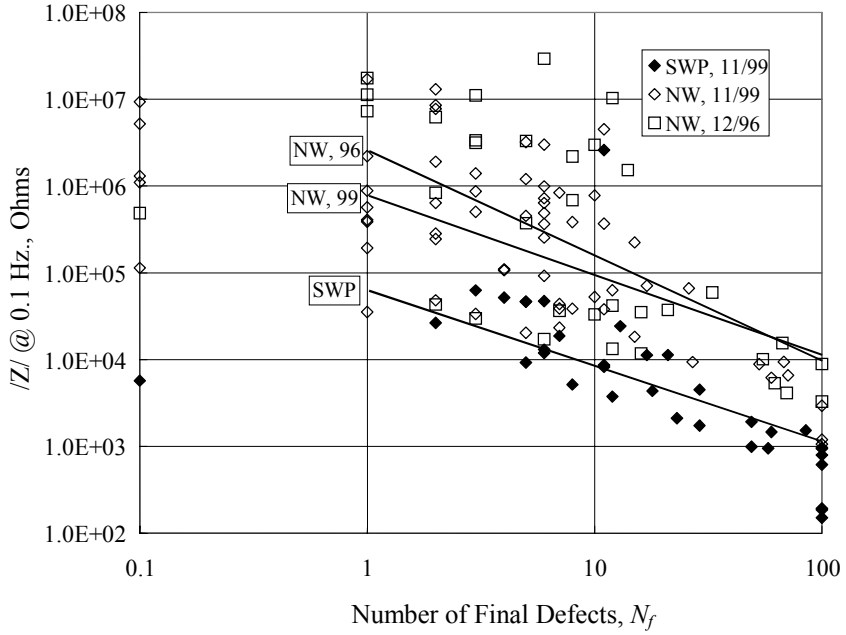

Figure 24: Plot of impedance versus the number of final defects for specimens from the third and fourth autopsies.

relationship between the number of final defects and macrocell current, as discussed above in conjunction with Figure 19.

Lastly, Figure 25 reproduces the data in Figure 24 for specimens from the fourth autopsy but with each data point identified according to bar source. This indicates that the coating on **U**

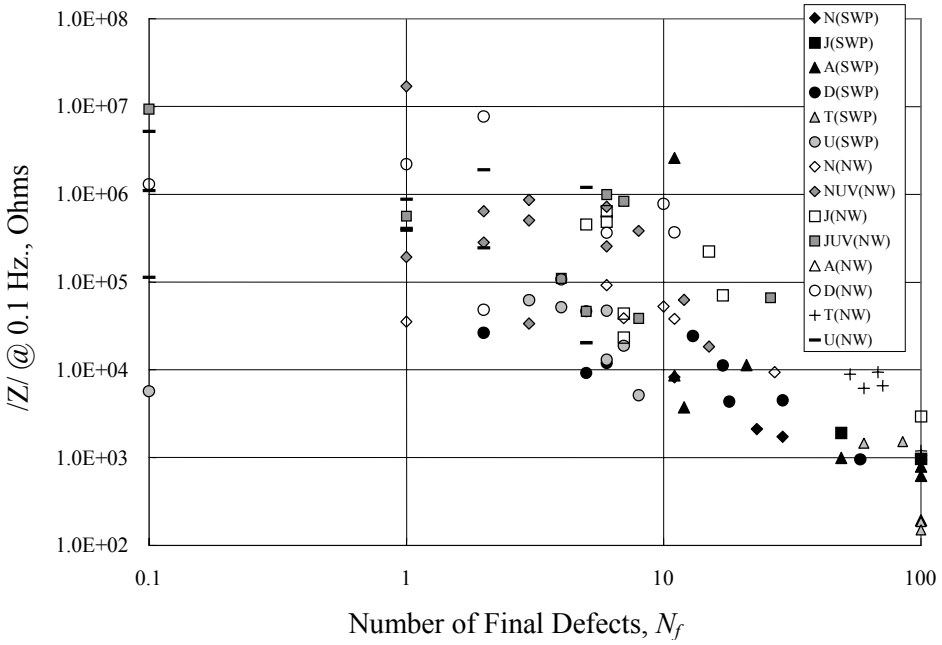

Figure 25: Plot of impedance @ 0.1 Hz. versus the number of final defects with the data identified according to bar source.

source bars, and to a lesser extent those of **D** source, afforded relatively high resistance to defect development for the SWP exposure. As noted above, these same bars performed well in the earlier NCHRP 10-37 tests (9).

PERFORMANCE OF PRE-WEATHERED VERSUS NON-PRE-WEATHERED BARS

As noted above, some ECRs were subjected to four months of natural weathering prior to their being cast into the concrete slabs. Some of these bars, while exposed to weathering, were shielded from UV, whereas others were not. The analysis of these bars subsequent to the four months of weathering that was performed as a part of NCHRP Project 10-37 (9) indicated the presence of rust spots, increased coating defects, and reduced coating adhesion compared to non-exposed bars (9). However, no distinction between bars that were subjected to UV and those that were not was apparent. Consequently, bars of both types (pre-weathered with and without UV exposure) were treated as the same in the present evaluation. In this regard, Figure 25 indicates that impedance for pre-weathered bars was generally no worse than for non-exposed bars. Also, Table 8 lists the ratio of the final-to-initial number of coating defects for pre-weathered and non-exposed bars from the same source, as recorded from the third and fourth autopsies (one coating defect was assumed in cases where there were none and data for two non-pre-weathered bars with an excessive number of final defects were disregarded). In all cases the defect ratio was greater for the pre-weathered compared to the non-pre-weathered bars, which seems inconsistent with the performance results (Figure 25). However, as it turned out, the number of initial defects was relatively small for the pre-weathered bars, as indicated by Table 9; and this proportionally affected the final number of defects and, hence, bar performance. Apparently, the bars that were selected for pre-weathering were of abnormally high quality (few coating defects). Irrespective of this qualification, no abnormal adhesion loss or other adverse effect was apparent for the pre-weathered bars compared to the non-pre-weathered ones that were recovered from the long-term exposure slabs. However, it should be realized that the pre-weathered bars did develop additional coating defects. Consequently, performance would presumably have been better without the pre-exposure since the defect density would have been less.

Table 8: Ratio of final-to-initial coating defects for UV exposed bars.

	Third Autopsy	Fourth Autopsy
N_f/N_i (**N**: Non-Exposed)	1.1	1.5
N_f/N_i (**N**: Weathered)	12.8	3.7
N_f/N_i (**J**: Non-Exposed)	3.9	2.0
N_f/N_i (**J**: Weathered)	25.8	3.4

Table 9: Number of initial coating defects for weathered and non-weathered ECRs from sources **N** and **J**.

	N_i (Third Autopsy)	N_i (Fourth Autopsy)
N (Non-Exposed)	8	13
N (Weathered)	1	1
J (Non-Exposed)	5	7
J (Weathered)	0	2

CHAPTER 3

INTREPRETATION, APPRAISAL, AND APPLICATION

COATING DEFECTS

Performance of the test slab ECRs was governed primarily by the coating defect density, which, for the as-received bars, varied from few or nil to excessive (too high to count). This was in spite of the fact that the bars were acquired for research purposes. Bars in the former category (few or nil coating defects) probably reflect what can be achieved under laboratory conditions with careful handling, whereas the latter (excessive defects) may be indicative of what results for ECRs that are placed in conjunction with actual construction projects. In this regard, a recent study has reported the average in-place coating defect density for ECRs in bridge decks just subsequent to concrete pouring as approximately one per inch (11).

Coating disbondment originated at coating defects in conjunction with either anodic or cathodic processes, or both, and spread outward over time therefrom. Consequently, the extent of coating disbondment was proportional to the number of coating defects (see Figures 17 and 18).

The number of coating defects increased during exposure. For slabs exposed to natural weathering, this increase was by a factor of $0.4 \cdot N_i$ per bar year (Equation (1)). In the case of salt water ponded specimens, however, the number of coating defects increased almost seven time more rapidly than for natural weathering such that $2.7 \cdot N_i$ additional defects developed on average per bar per year (Equation (2)). Consequently, the number of additional defects depended upon exposure condition and the initial number of defects. The latter finding; that is, that the final defect number was a function of the initial number, may reflect properties of the coating rather than the initial number of defects per se. In other words, the coating property or properties that caused few versus many initial coating defects may have proportionally affected the number of defects that formed during the exposure. These observations are generally consistent with previous impedance measurements performed upon the same source bars during accelerated hot water testing (9).

The critical defect density for the present bars above which disbondment and macrocell current were relatively high was approximately one defect per inch of bar length. While this exceeds what is presently specified by standards that pertain to ECR (one coating defect per linear foot), the latter criterion is invariably applied just after the coating operation and, accordingly, does not address defects that form during handling, packaging, shipping, storage, and placement. As noted above, the average in-place coating defect density just after concrete pouring has been reported as approximately one defect per inch of bar length (11), which is the same as the demarcation coating defect density determined in the present study.

SERVICE LIFE PROJECTION

Based upon the observations reported in Chapter 2, an analysis was performed to project the likely service life* of concrete reinforced with ECR. This assumed that the time-to-corrosion induced cracking and spalling is comprised of three component times, as listed below:

---

* For the present discussion, the term “service life” is defined as the time at which significant corrosion and probably cracking and spalling occur. A quantitative definition for the purpose of the present analysis is provided subsequently.

1. The time subsequent to initial exposure, designated T_1, for a critical chloride concentration to develop at the ECR depth.

2. The time subsequent to chloride contamination, designated T_2, for a coating defect density of one per inch of bar length to occur.

3. A period of subsequent ECR corrosion, designated T_3, that leads to concrete cracking and spalling.

Thus,

$$T_t = T_1 + T_2 + T_3. \quad (3)$$

Because the present ECR test slabs contained a relatively high concentration of admixed chlorides, the first of these times (T_1) was circumvented. In situations where the concrete is not initially chloride contaminated, T_1 can be determined based upon a Fick's second law analysis and assuming values for 1) surface chloride concentration, 2) critical chloride concentration to initiate corrosion, and 3) steel depth. The second period, T_2, was also zero for bars where $N_i \geq 14$ (one or more defects per inch); and life in these cases was determined solely by T_3. Otherwise ($N_i \leq 14$), both T_2 and T_3 influenced longevity. The time T_3 was assumed to end and service life to be reached when a net steel penetration of 25 μm occurred (12,13). This corresponds to a charge transfer of approximately 2 $\mu A \cdot$ years

Based upon the above, T_2 is projected by setting N_f in Equations (1) and (2) to 14. Thus,

$$T_2 = 2.5 \cdot \left(\frac{14}{N_i} - 1 \right) \text{ and} \quad (4)$$

$$T_2 = 0.37 \left(\frac{14}{N_i} - 1 \right), \quad (5)$$

for the NW and SWP exposures, respectively. Tables 10 and 11 tabulate values for T_2 as a function of N_i (initial coating defects per 14 in. long bar) and N_i' (initial coating defects per foot), for the NW and SWP exposures, respectively. This shows the duration of this life

Table 10: Time for a coating defect density of one per in. to develop upon NW exposure as a function of the initial defect density.

N_i (per bar)	N_i' (per ft)	T_2, years
0.1	0.1	347.5
0.5	0.4	67.5
1.2	1.0*	26.7
2.3	2.0	12.5
4.0	3.4	6.3
8.0	6.9	1.9
14.0	12.0	0.0
28.0	24.0	0.0

* Corresponds to the present specification.

Table 11: Time required for a coating defect density of one per in. to develop upon SWP exposure as a function of the initial defect density.

N_i (per bar)	N_i' (per ft)	T_2, years
0.1	0.1	52.1
0.5	0.4	10.1
1.2	1.0*	4.0
2.3	2.0	1.9
4.0	3.4	0.9
8.0	6.9	0.3
14.0	12.0	0.0
28.0	24.0	0.0

* Corresponds to the present specification.

component for minimum specification bars (one coating defect per foot) to be approximately 27 years for the NW exposure and four years for SWP. For an average in-place coating density of one per inch (11), T_2 is zero in both environments.

From Figure 19, equations relating N_f and macrocell current density, i, for the T_3 regime ($N_i \geq 14$) are,

$$N_f = 31.8 \cdot \log i + 132.4 \quad \text{and} \tag{6}$$

$$N_f = 47.2 \cdot \log i + 87.0\,, \tag{7}$$

for NW and SWP, respectively. Substitution of Equation 1 into 6 and Equation 2 into 7, respectively, and rearranging yields,

$$i = 10^{\left(\frac{N(0.4 \cdot T + 1) - 132.4}{31.8}\right)} \quad \text{and} \tag{8}$$

$$i = 10^{\left(\frac{N(2.67 \cdot T + 1) - 87.0}{47.2}\right)}, \tag{9}$$

for the NW and SWP cases, respectively, where in these expressions N_i has been set equal to the number of coating defects at the end of T_2 (N_2). Upon multiplying both sides by T, the time at which $i \cdot T = 2\,\mu\text{A} \cdot \text{years}$ (T_3) is determined. Tables 12 and 13 list the net charge that is transferred as a function of time and indicate that this requires 16 years for the NW exposure and approximately two years with SWP. Situations where $N_i > 14$ can be treated by substituting this value (14) for N_2.

The total time for the second and third periods was calculated as T_2 plus T_3. Table 14 provides the results for the NW exposure and Table 15 for the SWP. Thus, a service life for the ECR reinforced concrete slabs subsequent to the threshold chloride concentration being reached and based upon the above damage criterion (25 μm metal loss) is projected to vary from 46 to 16 years for the NW exposure as defect density increases from the specification value (one per foot)

to one per inch. In the SWP case, the corresponding time (T_2 plus T_3) is from 6.5 to 2.0 years. Figure 26 provides a graphical representation of the Table 14 and 15 data.

Table 12: Listing of the time for various charge transfers to occur for ECR during the NW type exposure.

T_3 (post N=14)	Charge Trans., μA*years
1	0.0003
5	0.0072
10	0.11
15	1.24
16	1.99

Table 13: Listing of the time for various charge transfers to occur for ECR during the SWP type exposure.

T_3 (post N=14)	Charge Trans., μA*years
1.00	0.18
1.50	0.66
1.75	1.21
1.97	2.03

Table 14: Listing of the time for periods two and three and the sum of these two times as a function of the defect density at the beginning of period two for the NW exposure.

N_i, per bar	N_i`, per ft	T_2, years	T_3, years	$T_2 + T_3$, years
0.1	0.1	347.5	16	363.5
0.5	0.4	67.5	16	83.5
1.2	1.0	30.3	16	46.3
4	3.4	6.3	16	22.3
8	6.9	1.9	16	17.9
14	12.0	0	16	16.0
28	24.0	0	16	16.0

Experience from the Florida Keys bridges (3-6) is consistent with the SWP results in that, first, several years were projected for the substructure concrete at the steel depth to become chloride contaminated (the T_1 term in Equation (5)) and, second, the total time for initial cracking and spalling was six years (3-6). Performance of the present slabs and of actual structures is expected to decrease with increasing 1) temperature, 2) time-of-wetness (provided the concrete is not continuously water saturated), 3) concrete chloride concentration (concrete resistivity should decrease with increasing chlorides and macrocell current should increase proportionally), and 4) rate of subsequent salt applications. At the severe end of service exposure conditions, performance is thought to approach that of the SWP condition and the Keys bridges exposure. As

Table 15: Listing of the time for periods two and three and the sum of these two times as a function of the defect density at the beginning of period two for the SWP exposure.

N_i, per bar	N_i', per ft	T_2, years	T_3, years	$T_2 + T_3$, years
0.1	0.1	52.1	2.0	54.1
0.5	0.4	10.1	2.0	12.1
1.2	1.0	4.0	2.0	6.0
4.0	3.4	0.9	2.0	2.9
8.0	6.9	0.3	2.0	2.3
14.0	12.0	0.0	2.0	2.0
28.0	24.0	0.0	2.0	2.0

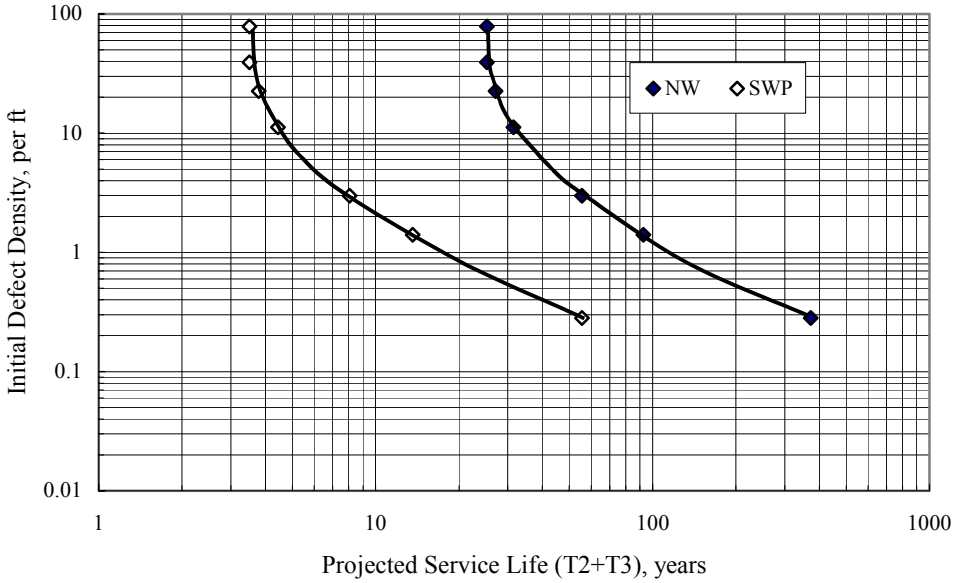

Figure 26: Plot of T_2 plus T_3 service life versus the number of coating defects for the NW and SWP exposures.

conditions moderate, however, performance should improve and perhaps even exceed that represented by the NW exposure. It must be kept in mind, however, that the above analysis (Tables 14 and 15 and Figure 26) disregards any contribution from the T_1 component of service life. On the other hand, T_1 is likely to be adversely affected (minimized) by deck cracking above ECRs, which is commonly observed on actual structures, as discussed above.

CHAPTER 4

CONCLUSIONS AND RECOMMENDATIONS

A six-plus year outdoor test yard exposure program was performed upon concrete slabs that were reinforced in an upper, chloride admixed lift with epoxy-coated steel and in the lower, chloride free lift using black steel. Bars from six different sources were employed; and coating properties, including thickness, hardness, and defect type and density, were determined prior to casting. Coating performance data from several different accelerated tests are available for these same materials from a preceding program (9). The initial 2.7 years of exposure consisted of potable water ponding according to four different wet-dry cycles. Subsequently, the slabs experienced natural weathering only but with some subjected to predominantly wet ponding with a 15 percent NaCl solution for the final 13 months. Specimen monitoring consisted of periodic measurement of potential, macrocell current, and modulus of impedance @ 0.1 Hz. The exposures were terminated and slabs autopsied at various times; and the number of final coating defects, adhesion, extent of coating disbondment, and chloride concentration at the steel depth were determined. Based upon this, the following conclusions were reached:

1. Coating defect density was the predominant parameter that affected ECR performance. The number of initial coating defects for bars in the test slabs varied from few or nil to excessive (greater than 100 per bar length (14 inches)) depending upon bar source.

2. The number of coating defects increased with increasing exposure time with the rate of this increase being constant and proportional to the initial defect density or, alternatively, to bar source such that the ratio of the final-to-initial number of defects was roughly constant for a given type of exposure (natural weathering versus salt water ponding). This ratio was, on average, approximately seven times greater for salt water ponded specimens compared to naturally weathered ones.

3. Concrete cracks developed above the ECRs during the course of the exposures; and although corrosion apparently contributed to widening and lengthening of these with time, this was not the cause of their occurrence. No cracks that were attributable to corrosion were disclosed. Black bar control slabs, on the other hand, exhibited relatively wide cracks of the same type (non-corrosion induced) initially; and these slabs spalled and fell apart during the course of the exposures.

4. Coating disbondment occurred at and proceeded outward from coating defects. The extent of this disbondment relative to the net bar surface area was proportional to the number of coating defects.

5. In general, potential was more active, macrocell current was higher, and impedance was lower the greater the number of coating defects and the more extensive the disbondment. The last of these observations suggests that it may be feasible to assess the coating defect density on in-place bars in terms of non-destructive measurement of the specific impedance at 0.1 Hz.

6. Corrosion occurred at coating defects and at locations beneath the disbonded coating that were anodic. Such corrosion ranged from extensive for ECRs with a large number of coating defects and disbondment, particularly if these were salt water ponded, to nil in cases where coating defect density was low. A defect density of about one per inch of bar length was the

demarcation between acceptable and non-acceptable corrosion performance. This critical defect density pertains, however, to the in-place coating condition and, as such, applies after any bar fabrication, handling, packaging, shipping, storage, and placement. In view of the findings of a recent study that reported an average coating defect density on ECRs just after concrete placement of approximately one per inch (11), it can be reasoned that one-half of all bridge structures have a defect density equal to or in excess of this critical value at the time of commissioning.

7. ECRs that were pre-exposed at a near-ocean atmospheric site for four months developed rust spots and additional coating defects beyond those that were present in the as-received condition. Performance was presumably less than if these additional defects had not formed, although it was the same as for non-exposed bars with the same defect density. No affect of ultraviolet exposure for this same time period (four months) was disclosed.

8. The ECRs from one of the six sources were provided with a chromium conversion coating prior to epoxy-coating. These bars exhibited a low initial coating defect density; and corrosion performance was good, although no better than for non-conversion coated bars with the same defect density. It could not be determined if the chromium conversion coating was responsible for the low initial coating defect density.

9. A service life model for ECR reinforced concrete was developed and applied to each of the two types of exposure. This is based upon three component times as,

   A. The time subsequent to initial exposure, designated T_1, for a critical chloride concentration to develop at the ECR depth.

   B. The time, designated T_2, subsequent to chloride contamination for a coating defect density of one per inch of bar length to develop.

   C. A period, designated T_3, subsequent to development of a coating defect density of one per inch during which corrosion is ongoing and leads ultimately to concrete cracking and spalling.

   The time associated with Period A can be determined from a Fick's second law analysis. However, a common observation is that non-corrosion induced concrete cracks develop above ECRs in bridge decks. Where this is the case, the time T_1 may be considerably shortened and a Fick's second law analysis inapplicable. Duration of Period B varies inversely with the density of initial coating defects such that, as this density increases from the specification value (one per foot) to one per inch, T_2 decreased from 30 to zero years for the natural weather (NW) exposure and from four to zero years for the salt water ponding (SWP). The fact that a recent study has reported an average in-place coating defect density of one per inch (11) suggests that a critical assessment should consider that $T_2 = 0$ for 50 percent of the existing ECR bridge population. On the other hand, T_3 was projected as 16 years for the NW exposure and 2.0 years for the SWP. Thus, subsequent to chloride contamination, the remaining service life for the NW exposure decreases from 46 to 16 years and for the SWP from 6.0 to 2.0 years as the density of coating defects increases over the above range (specification value of one per foot to one per inch). Such a result for the SWP exposed slabs is consistent with that of the Florida Keys bridge substructures, indicating an apparent equivalence in the two exposures. On the other hand, environmental exposure severity for northern bridge decks subject to deicing salts is likely to vary according to temperature, time of wetness, and frequency of salt applications.

As a consequence of this research, the following recommendations are made:

1. The service life model that was developed projected ECR performance for two exposure severities; however, only one of these has been calibrated with actual service. Recognizing that ECR performance should decrease with increasing 1) temperature, 2) time-of-wetness (this assumes that the concrete is not continuously water saturated), 3) concrete chloride concentration, and 4) rate of subsequent salt applications, a study should be commissioned to expand the model from the two exposures to a continuum and calibrate this with North American longitudes and latitudes and salting practice. A companion study is recommended to determine the coating defect density for bars in existing bridges as a function of age and exposure severity as defined by the above variables (temperature, time-of-wetness, concrete chloride concentration, and frequency of salt applications). It may be feasible to accomplish this using impedance measurements.

2. The finding that coating defect density is the most important ECR performance parameter for bars that otherwise conform to specification and that the average in-place defect density in new bridge decks is approximately one per inch (11) indicates that efforts by states to enhance long-term durability should focus upon methods whereby a) the time to occurrence of the threshold chloride concentration at the steel depth (the T_1 term in Equation (3)) can be increased* and b) the coating defect density of in-place ECRs for new construction can be reduced.

---

* Enhancement of T_1 may not be feasible or the enhancement minimal in situations where concrete cracking above ECRs occurs or is anticipated.

REFERENCES

1. Clifton, J.R., Beeghley, H.F., and Mathey, R.G., "Non-Metallic Coatings for Reinforcing Bars," Report No. FHWA-RD-74-18, PB No. 236424, Federal Highway Administration, Washington, D.C., February, 1974.

2. Clear, K.C. and Virmani, Y.P., "Corrosion of Non-Specification Epoxy-Coated Rebars in Salty Concrete," Paper No. 114 presented at CORROSION/83, April 18-22, 1883, Anaheim, CA.

3. Powers, R.G. and Kessler, R., Corrosion Evaluation of Substructure, Long Key Bridge," Corrosion Report No. 87-9A, Florida Department of Transportation, Gainesville, FL, 1987.

4. Powers, R.G., "Corrosion of Epoxy-Coated Rebar, Keys Segmental Bridges Monroe County, Report No. 88-8A, Florida Department of Transportation, Gainesville, FL, August, 1988.

5. Zayed, A.M. and Sagues, A.A., "Corrosion of Epoxy-Coated Reinforcing Steel in Concrete," Paper No. 386 presented at CORROSION/89, New Orleans, LA, April 21, 1989.

6. Gustafson, D.P., "Epoxy Update," Civil Engineering, Vol. 58, No. 10, pp. 38-41, 1988.

7. "Effectiveness of Epoxy-Coated Reinforcing Steel," Final Report submitted to Concrete Reinforcing Steel Institute by K. C. Clear, Inc., December, 1991.

8. "Effectiveness of Epoxy-Coated Reinforcing Steel," Final Report submitted to Canadian Strategic Highway Research Program by K. C. Clear, Inc., December, 1992.

9. Clear, K.C., Hartt, W.H., McIntyre, J.F., and Lee, S.K., "Performance of Epoxy-Coated Reinforcing Steel in Highway Bridges," NCHRP Report No. 370, National Cooperative Highway Research Program, Washington, D.C., 1995.

10. ASTM C 1218 "Standard Test Methods for Water-Soluble Chloride in Mortar and Concrete," ASTM Annual Book of Standards, American Society of Testing and Materials, Philadelphia, 1997.

11. Samples, L.M., Ramirez, J.A., "Field Investigations of Existing and New Construction Concrete Bridge Decks," School of Civil Engineering, Purdue University report reprinted by the Concrete Reinforcing Steel Institute as CRSI Research Series 6.

12. Spellman, D.L. and Stratfull, R.F., "Laboratory Corrosion Test of Steel in Concrete," Research Report No. M&R 635116-3, Materials and Research Department, California Division of Highways, September, 1968.

13. Berke, N.S. and Sundberg, K.M., “The Effects of Admixtures and Concrete Mix Designs on Long-Term Concrete Durability in Chloride Environments,” paper no. 386 presented at CORROSION/89, New Orleans, April 17-21, 1989.

APPENDIX

SPECIMENS AND EXPERIMENTAL PROCEDURE

EPOXY-COATED REINFORCEMENT

The ECRs were acquired from six different sources including one U.K. supplier and identified as **A**, **D**, **J**, **N**, **T**, and **U**. In the case of the U.K. bars, a chromate conversion coating was employed as part of the coating application, while no such pre-treatment was used for the others. Characteristics of these coatings, including 1) number of defects, holidays, and bare areas, 2) hardness, and 3) thickness, were determined. Also, measurements and tests such as 1) solvent weight loss, 2) impedance upon hot water exposure, 3) Accelerated Corrosion Testing (ACT), and 4) adhesion were performed with results from these being presented previously (A1) and summarized here in Table A-1. Because of scheduling and acquisition difficulties, bars from each source did not undergo all tests. A general conclusion from the initial study (A1) based upon these data was that there was a lack of correlation between performance of bars from a given source in the different tests. An exception was that bars that exhibited low solvent extraction weight loss tended to perform well in the Hot Water Test. The former behavior (low solvent extraction weight loss) is indicative of a relatively low amount of plasticizer and a high degree of cross-linking. Such coatings are expected to have relatively few conductive pathways and reduced porosity, which was projected to promote good performance in the Hot Water Test. It was also noted, however, that coating defects contributed to poor performance because these facilitated anodic undermining and cathodic disbondment. It was concluded that the highest quality bars; that is, ones that exhibited capacitive behavior as determined by electrochemical impedance spectroscopy (EIS), low solvent extraction weight loss, and no coating defects, may perform satisfactorily in long-term service.

Table A-1: Summary of properties for the different epoxy coatings.

Type of Test	Ranking		
	Good	Intermediate	Poor
DW/HWT/EIS* (Capacitive**)	**U**, **D**, **N**	**A**	**J**
DW/HWT/EIS* (As Received***)	**U**, **N** > **D** > **A** > **J** > **T**		
ACT	**U** > **J** > **D** > **N**		
Coating Thickness****	Thickest		Thinnest
	A, **N** > **D** > **U** > **T**		
Solvent Extraction Weight Loss	Low		High
	A, **D**, **U**	**T**, **J**	
Coating Defects/Holidays	**T** > **N** > **A** > **J** > **D** > **U**		
Post HWT Adhesion	**T** > **U** > **D** > **J** > **A** > **N**		

* DW-Distilled Water; HWT - Hot Water Test; EIS - Electrochemical Impedance Spectroscopy

** Capacitive: Defect free bars..

*** As Received: Bars containing defects.

**** Coating thickness on all bars was within specification.

Some **J** and **N** bars (designated as **JUV** and **NUV**) were subjected to four months of outdoor exposure prior to these being incorporated into slabs. One group of these, while exposed to weathering, was shielded from UV, whereas the second group was fully exposed. Post-outdoor exposure testing indicated that coating adhesion was lower than for non-exposed bars and that additional holidays and rust spots had developed. Also, the average 0.1 Hz impedance upon hot water testing was relatively low. No distinction was apparent, however, between pre-weathered bars that experienced UV and those that were exposed but shielded from UV.

CONCRETE TEST SLABS

As noted above, 76 concrete slabs containing ECR and 12 controls (black bars only) were fabricated in October, 1992. These were 35.6 cm (14.0 in) long by 33.0 cm (13.0 in) wide by 17.8 cm (7.0 in) thick, as illustrated schematically in Figure A-1. Length of the UV bars was 15.2 cm (6.0 in) with two of these being mounted together end-to-end using a plastic pipe section such

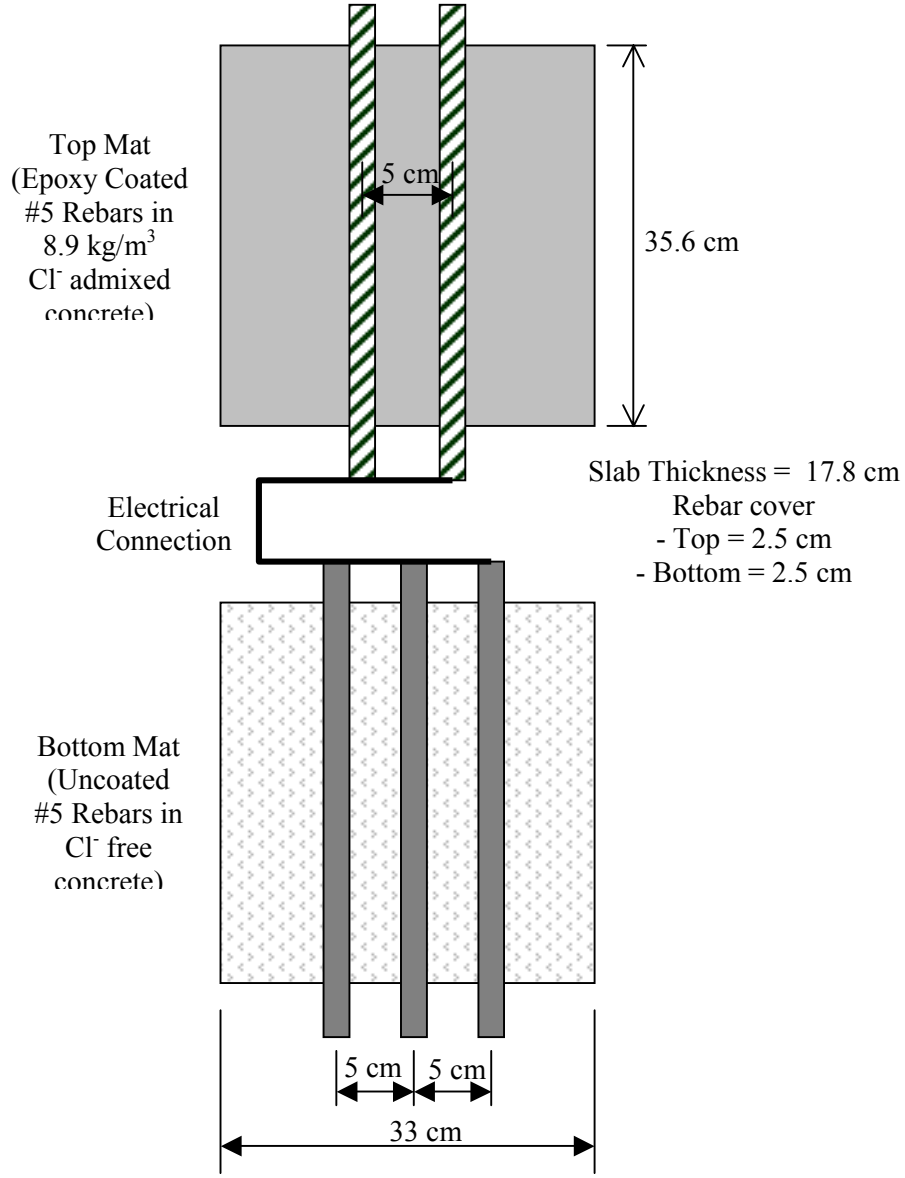

Figure A-1: Geometry of test slabs.

Table A-2: Concrete mix design for test slabs.

Constituent	Content
Cement	356.7 kg/m^3
Water	178.4 kg/m^3
Coarse Aggregate	910.3 kg/m^3
Fine Aggregate	823.5 kg/m^3
Daravair, AEA	38.7 ml/m^3

that a single test bar resulted. The upper 5 cm (2 in) of each slab was comprised of 0.5 w/c concrete containing 8.9 kg/m^3 (15 lb/yd^3) of admixed chlorides as $CaCl_2$ and two #5 ECR specimens from a given source (alternatively, four 6 in. long #5 pre-weathered ECRs) or black bars in the case of the control slabs). The bottom portion was prepared using chloride-free concrete of the same w/c and contained three #5 black bars. Table A-2 provides information pertaining to the concrete mix. The clear concrete cover for both rebar mats was 2.5 cm (1.0 in). A macrocell was established between the top and bottom bars through external electrical lead wire connections.

EXPOSURE

The slabs were exposed in an outdoor Florida Atlantic University test yard in Boca Raton, Florida approximately two miles (three km) inland from the Atlantic Ocean beginning in March, 1993. Figures A-2 and A-3 show photographs of specimens under exposure. For the initial 2.7 years, the slabs experienced natural weathering in conjunction with one of four different wet-dry cycles, as listed in Table A-3. During the summer, 1995 hairline cracks were detected upon the top slab surface of some specimens. The width and number of these cracks increased during the course of the exposure, as discussed subsequently. Based upon the observation that slab

Figure A-2: Photograph of specimens under exposure. The plastic cover is to protect cyclically ponded specimens from rain.

Figure A-3: Close-up photograph of specimens in Figure A-2.

Table A-3: Description of the different wet-dry cycles.

Cycle Designation	Description
A	3 days wet – 4 days dry
B	11 days wet – 3 days dry
C	1 day wet – 13 days dry
D	Continuously wet

performance was independent of the type of ponding cycle (Table A-3), cyclic ponding was discontinued in September, 1995; and the slabs remained under natural weathering exposure only. Then, in October, 1998 an accelerated exposure that involved repetitive 12 week periods of, first, one week wet-one week dry and, second, continuous ponding, both with 15 weight percent NaCl, was instituted for 17 of the 44 remaining slabs. The other slabs continued under natural weathering exposure. Selection of slabs for the accelerated versus continued natural weathering exposure was such that both "good" and "poor" performers," based upon macrocell current, were included in each category. Table A-4 lists specimens according to the two types of exposure.

SPECIMEN CHARACTERIZATION AND MONITORING

At periodic intervals throughout the exposures, measurements were made of 1) open circuit potential (OCP), 2) macrocell current, and 3) modulus of impedance (log /*Z*/ at 0.1 Hz). The initial data that were acquired in 1993 served as a baseline to which subsequent results were compared.

AUTOPSY PROCEDURE

As noted above, exposure testing of certain specimens was terminated at different times in the program; and these specimens were autopsied and condition of the ECR determined. Table A-5 lists the schedule for each autopsy, the specimens that were involved, and the purpose. Correspondingly, Table A-6 defines the autopsy procedure that was followed in each case.

Table A-4. Test Matrix for Salt Water Ponding and Natural Weathering Exposures.

Source	Salt Water Ponded Specimens		Natural Weathering Specimens	Total Specimens per Source
	Good Performers	Poor Performers		
N	#5, #7	-	#3, #6, #8	5
NUV	-	-	#9, #11, #12	3
J	#16	-	#15, #18, #20, #22	5
JUV	-	-	#26, #27	2
A	#29, #36, #40	#31	#34, #37, #39	7
D	#41, #43, #48	#52	#45, #46, #47, #50	8
T	#53	#63	#54, #61, #62	5
U	#68, #71, #73	#66	#67, #69, #74, #75, #76	9
Total Spec. per Exposure	13	4	27	44

Table A-5: Autopsy information and schedule.

Autopsy Number	Date	Number of ECR Slabs Autopsied	Exposure Duration, years	Purpose of Autopsy
1	Oct., 1993	7	0.8	Provide information for Project 10-37 final report.
2	Dec., 1995	3	2.7	To investigate the cause of cracks that had formed on some slabs.
3	May., 1996	22	3.7	To define condition and determine need for continued exposure.
4	Nov., 1999	44	6.7	To characterize specimens at completion of the exposure program.

Table A-6: Steps in the slab autopsy process.

Step	Task
1	Slabs broken open and the bars extracted.
2	Concrete/rebar interfaces examined for corrosion products.
3	Coating defects located visually and with a M-1 holiday detector.
4	Defect sites identified and marked on the bar with an indelible pen.
5	Defect types identified and counted using a magnifier and stereomicroscope.
6	Defect locations recorded on an autopsy mapping sheet.
7	Photographs taken of both sides of each bar.
8	Disbonded coating removed beginning from defect sites using a utility knife.
9	Knife adhesion tests performed at undamaged coating areas (typically six spots per bar).
10	Upon removal of the delaminated coating, a second set of photographs was taken.
11	The extent of coating disbondment was measured.

Figure A-4 is a photograph of the first autopsy step where the ECRs were extracted by cutting along the joint between the top and bottom lifts using a gas powered masonry saw. Figure A-5 shows a specimen subsequent to this saw cutting where the two specimen halves have been physical separated along the concrete lift, and Figure A-6 illustrates the method for cracking open the upper lift along the ECR length using a chisel. The ECRs were then removed from the concrete and examined for coating defects and corrosion. Also, the bar traces in the concrete were examined for presence of corrosion products and for cracks. During autopsies 3 and 4, concrete powder samples were taken from the ECR/concrete and black bar/concrete interface of

Figure A-4: Photograph showing the initial step in autopsy of a specimen where a saw cut was made along the lift line.

Figure A-5: Photograph of specimen after breaking apart along the lift line.

Figure A-6: Photograph of the upper lift containing two ECRs being broken open.

some of the slabs by drilling with a 6.4 mm diameter masonry drill bit. A photograph of this step is shown in Figure A-7. These samples were used for determination of the water-soluble chloride content according to ASTM C-1218 (A2).

Figure A-7: Photograph of a concrete powder sample being taken by drilling at the reinforcement trace of a fractured specimen.

REFERENCES

A1. Clear, K.C., Hartt, W.H., McIntyre, J.F., and Lee, S.K., "Performance of Epoxy-Coated Reinforcing Steel in Highway Bridges," NCHRP Report No. 370, National Cooperative Highway Research Program, Washington, D.C., 1995.

A2. ASTM C 1218 “Standard Test Methods for Water-Soluble Chloride in Mortar and Concrete,” ASTM Annual Book of Standards, American Society of Testing and Materials, Philadelphia, 1997.